

Review

Open Access



MOFs as platforms for multiscale structural regulation: new frontiers in photocatalyst design

Jianqiao Liu^{1,#}, Zili Gong^{1,#}, Di Wu¹, Yuan Liu¹, Junsheng Wang¹, Qianru Zhang², Ce Fu¹

¹College of Information Science and Technology, Dalian Maritime University, Dalian 116026, Liaoning, China.

²Institute of Agricultural Resources and Regional Planning, Chinese Academy of Agricultural Sciences, Beijing 100081, China.

[#]Authors contributed equally.

Correspondence to: Prof. Junsheng Wang, College of Information Science and Technology, Dalian Maritime University, Linghai Road 1, Ganjingzi District, Dalian 116026, Liaoning, China. E-mail: Wangjsh@dmlu.edu.cn; Prof. Qianru Zhang, Institute of Agricultural Resources and Regional Planning, Chinese Academy of Agricultural Sciences, Zhongguancun South Street 12, Haidian District, Beijing 100081, China. E-mail: Zhangqianru@caas.cn; Prof. Ce Fu, College of Information Science and Technology, Dalian Maritime University, Linghai Road 1, Ganjingzi District, Dalian 116026, Liaoning, China. E-mail: fuce_dmlu@sina.com

How to cite this article: Liu, J.; Gong, Z.; Wu, D.; Liu, Y.; Wang, J.; Zhang, Q.; Fu, C. MOFs as platforms for multiscale structural regulation: new frontiers in photocatalyst design. *Microstructures* 2025, 5, 2025056. <https://dx.doi.org/10.20517/microstructures.2024.171>

Received: 24 Dec 2024 **First Decision:** 10 Feb 2025 **Revised:** 15 Feb 2025 **Accepted:** 27 Feb 2025 **Published:** 25 Apr 2025

Academic Editors: Yongfa Zhu, Chunqiang Zhuang **Copy Editor:** Fangling Lan **Production Editor:** Fangling Lan

Abstract

Photocatalysis plays a pivotal role in sustainable technology, driving pollutant degradation and energy conversion through solar-driven chemical reactions. However, conventional photocatalysts are limited by their structural tunability, hindering their adaptability to evolving photocatalytic applications. This underscores the urgent need for innovative approaches to overcome these challenges. Metal-organic frameworks (MOFs), with their tunable structures, offer a promising solution by overcoming these limitations. Here, we demonstrate a comprehensive overview of the structural regulation strategies in MOFs, emphasizing their evolution across multiple scales to enhance photocatalytic performance. This review begins by detailing the photoelectric and structural characteristics of MOFs and their development in structural regulation strategies for photocatalytic effectiveness. An in-depth analysis is undertaken into structural regulation strategies across multiple scales - macroscale, mesoscale, atomic-scale, and electronic-scale. The synergistic interactions among these levels are further explored, revealing their collective contribution to improved photocatalytic efficiency. These insights emphasize that the adaptable design strategies of MOFs serve as promising pathways for advancements in photocatalyst engineering. Finally, we examine the current photocatalytic applications of tunable structures in MOFs and provide perspectives on future challenges and advancements in this field. This review offers critical insights into MOF structural



© The Author(s) 2025. **Open Access** This article is licensed under a Creative Commons Attribution 4.0 International License (<https://creativecommons.org/licenses/by/4.0/>), which permits unrestricted use, sharing, adaptation, distribution and reproduction in any medium or format, for any purpose, even commercially, as long as you give appropriate credit to the original author(s) and the source, provide a link to the Creative Commons license, and indicate if changes were made.



regulation, highlighting its role in driving innovations in photocatalyst design and expanding photocatalytic technologies.

Keywords: Photocatalysis, metal-organic frameworks, multiscale structure, synergy, environmental/energy application

INTRODUCTION

Photocatalysis is a transformative technology that uses solar energy to drive chemical reactions, offering great potential for reducing environmental pollution and producing clean energy^[1-4]. Operating under mild conditions, photocatalysis leverages abundant solar energy to drive redox reactions, significantly reducing reliance on fossil fuels and lowering carbon emissions^[5-7]. It provides cost-effective solutions for degrading persistent pollutants in water and air, addressing pressing issues such as industrial wastewater treatment and the removal of volatile organic compounds^[8-10]. Applications in renewable energy production, including hydrogen generation through water splitting^[11,12] and carbon dioxide reduction into value-added fuels^[13,14], further underscore its pivotal role in the green energy transition^[15]. This versatility, driven by advancements in photocatalyst design, has led to significant improvements in reaction selectivity and efficiency, paving the way for industrial-scale adoption^[16-18]. The success of photocatalysis relies on the design of advanced photocatalysts, which govern its adaptability and effectiveness across diverse applications^[19-22].

Traditional photocatalysts face intrinsic limitations in structural tunability, restricting their adaptability to evolving application demands and hindering overall performance^[23-26]. The difficulty in fine-tuning their structures often leads to a low density of active sites, reducing the efficiency of photocatalytic reactions. Additionally, the lack of structural flexibility accelerates the recombination of photoexcited electron-hole pairs, significantly diminishing photocatalytic activity^[27,28]. Moreover, their inability to modify optical properties limits the absorption spectrum to a narrow range, restricting the effective utilization of solar energy under natural light conditions. Structural rigidity further complicates the integration of multiple active functionalities within a single material, reducing their capacity to perform complex or multi-step photocatalytic processes^[29,30]. As a result, many traditional photocatalysts struggle to maintain efficiency when transitioning from laboratory conditions to industrial applications, highlighting persistent scalability challenges^[31-33]. These shortcomings underscore the urgent need for innovative design strategies that enable precise structural control, enhance photocatalytic activity, and support the development of adaptable and scalable photocatalysts.

Characterized by their highly tunable structures and diverse functionalities, metal-organic frameworks (MOFs) have emerged as a promising class of choice to overcome the limitations of traditional photocatalysts^[34-36]. Their modular design allows for precise control over pore size, surface area, and chemical environments, optimizing light absorption and charge transfer processes^[37-39]. The incorporation of a wide range of metal nodes and organic linkers provides unparalleled flexibility in tailoring electronic properties for specific photocatalytic reactions^[40]. MOFs are also capable of integrating multiple active sites within a single framework, facilitating multi-step photocatalytic processes and significantly enhancing overall reaction efficiency^[41]. Their hierarchical porous structures promote efficient mass transport and improve accessibility to photocatalytic sites, which are critical for complex reactions and scalable applications^[42]. Furthermore, advancements in post-synthetic modification enable fine-tuning of MOF properties, such as stability and selectivity^[43], under diverse operational conditions. In recent years, MOF-based hybrids, such as MOF/covalent organic framework (COF)^[44] and the introduction of functional guests^[45] into MOFs, have garnered significant attention due to their enhanced photocatalytic performance.

Meanwhile, MOF-based derivatives have shown great potential in improving stability and forming unique structures^[46,47]. These hybrids and derivatives combine the tunability of MOFs with the superior properties of other materials^[48], significantly enhancing photocatalytic efficiency. These unique features position MOFs as a transformative platform for the rational design of next-generation photocatalysts, with potential to revolutionize applications in environmental remediation^[49,50] and renewable energy production^[51].

Here, this review focuses on the structural regulation of MOFs as a transformative strategy to address the limitations of conventional photocatalysts and advance their applications in sustainable technologies. It begins by introducing the photoelectric and structural characteristics of MOFs, emphasizing the features that establish them as ideal candidates for photocatalysis. The review then systematically explores structural regulation strategies across multiple scales - macroscale, mesoscale, atomic scale, and electronic scale - illustrating how each contributes to enhancing photocatalytic performance. Particular attention is given to the synergistic interactions across these scales, which provide valuable insights into the rational design of efficient and adaptable photocatalysts. The practical potential of MOFs is further demonstrated through their applications in environmental remediation and renewable energy production, underscoring their versatility in addressing diverse photocatalytic challenges. Additionally, recent advancements in post-synthetic modification techniques are analyzed, highlighting their role in optimizing stability, selectivity, and photocatalytic efficiency under various operational conditions. This comprehensive review not only offers a detailed examination of MOF-based structural regulation but also provides critical insights to guide the development of next-generation photocatalysts and expand the boundaries of photocatalytic technologies.

PROPERTIES OF MOF PHOTOCATALYSTS

Photoelectric properties

MOFs have become highly promising photocatalysts due to their ability to facilitate various photochemical reactions^[52]. During photocatalysis, they absorb photons, generating electron-hole pairs. Upon photon absorption, electrons are excited from the highest occupied molecular orbital (HOMO) or valence band (VB) to the lowest unoccupied molecular orbital (LUMO) or conduction band (CB), leaving holes behind^[53]. These charge carriers then separate and migrate to active sites within the framework, where they drive redox reactions^[54]. The efficiency of this process depends on several factors, including charge carrier generation rates, separation dynamics, transport efficiency, and recombination suppression.

Since Alvaro *et al.* first demonstrated the semiconducting properties of MOFs and their internal charge transfer mechanisms, they have received significant attention for photocatalytic applications^[55]. MOFs exhibit unique charge transfer pathways, primarily ligand-to-metal charge transfer (LMCT) and ligand-to-cluster charge transfer (LCCT), both of which enhance charge separation and suppress recombination [Figure 1]. LMCT occurs when electrons are transferred from the π -orbitals of organic linkers to the d-orbitals of metal nodes^[56]. This mechanism is especially prominent in MOFs featuring transition metal centers such as Ti or Fe. These metal nodes serve as active sites for reduction reactions. LMCT not only broadens the light absorption spectrum but also facilitates the activation of electron acceptors like O₂ or CO₂, thereby significantly improving photocatalytic performance^[57]. LCCT is characteristic of MOFs containing metal-oxo clusters, such as MOF-5 and UiO-series^[58,59]. In this mechanism, electrons are transferred from organic linkers to the entire metal cluster rather than a single metal atom. This delocalized charge transfer minimizes recombination rates and ensures stable electron transport throughout the framework, further enhancing photocatalytic efficiency. In addition to these pathways, metal-to-ligand charge transfer (MLCT)^[60] and Intra-ligand charge transfer (ILCT)^[61] can also contribute to the photocatalytic process by providing additional pathways for charge separation.

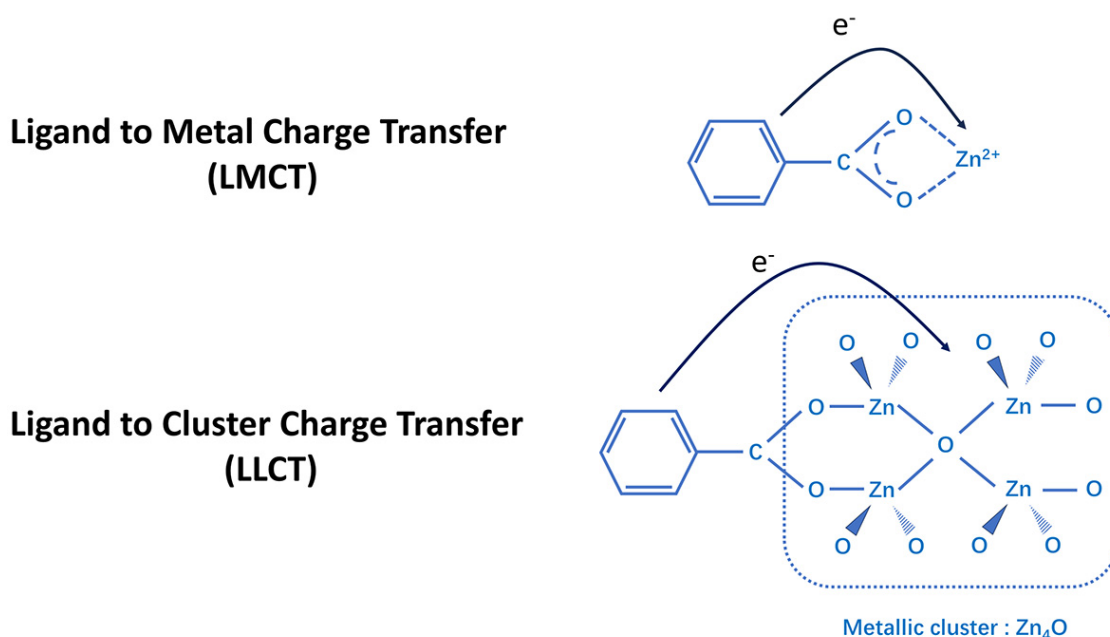


Figure 1. Charge transfer mechanisms in MOF-5.

The light absorption properties of MOFs are closely related to their HOMO and LUMO energy levels, which determine their bandgap^[62]. The HOMO is typically associated with the π -orbitals of organic linkers, while the LUMO is associated with the d-orbitals of metal nodes or clusters. The energy difference between these levels dictates the spectrum of light the photocatalysts can absorb. Depending on the combination of linkers and metal nodes, MOF bandgaps are highly tunable. Chemical modifications enable precise tuning of HOMO and LUMO energy levels. Substituents on organic linkers, such as electron-donating or electron-withdrawing groups, can shift HOMO and LUMO positions to optimize light absorption and photocatalytic activity^[63]. The combination of tunable HOMO-LUMO levels, multiple charge transfer mechanisms, and synergistic structural effects positions MOFs as an excellent direction for tackling photocatalytic challenges.

Structural properties

MOFs comprise two primary components: metal-based nodes and organic linkers^[64,65], which are connected through coordination bonds to form periodic and modular architectures [Figure 2A]. The metal-based nodes, often consisting of single metal ions or metal-oxo clusters, act as primary centers for electronic and structural functionality^[66]. Transition metals such as Ti, Zr, and Fe are commonly used, contributing to both photocatalytic activity and the robustness of the framework. In addition, the size, charge, and coordination environment of the metal nodes significantly influence the performance in different applications. Metals with higher charge, such as Ti^{4+} or Zr^{4+} , often result in greater framework stability, while more reactive metals, such as Fe^{3+} , enhance catalytic activity^[67]. Organic linkers, typically containing functional groups such as carboxylates, phosphonates, or imidazolates, provide structural connectivity and define the electronic properties of the MOFs^[68]. These linkers also create highly ordered porous structures with tunable pore sizes and surface functionalities, enabling MOFs to accommodate a wide range of photocatalytic applications. For example, linkers with conjugated π -electron systems, such as terephthalic acid or porphyrins, enhance light absorption and facilitate charge transfer^[69]. Some advanced linkers, such as 3-amino-1,2,4-triazole (Atz)^[70] and the bi-linker with 1,2,4,5-benzenetetracarboxylic acid (BTC) and 2-methylimidazole ($\text{C}_4\text{H}_6\text{N}_2$)^[71], are also contributing to the expansion of linker selection.

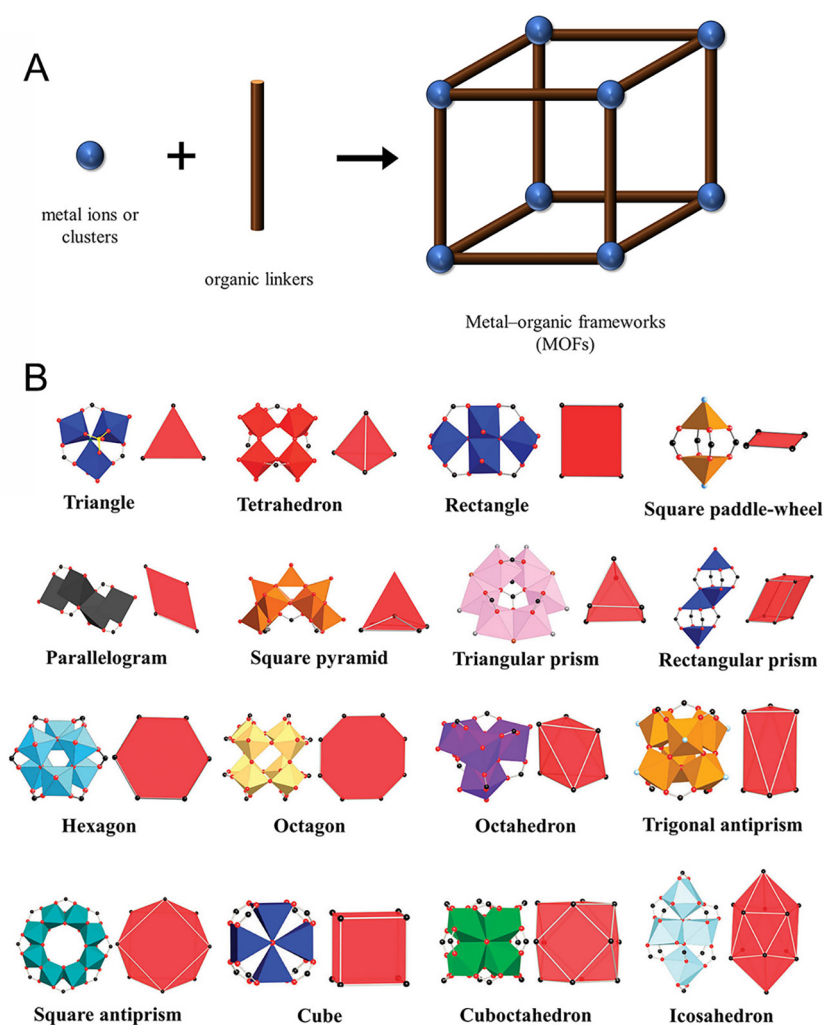


Figure 2. (A) Structural composition of MOFs; (B) Examples of some secondary building units (SBUs). Reproduced with permission Ref. [72] Copyright 2023 Elsevier.

Understanding the exact construction of MOFs based on metal ions and ligands is challenging due to their intricate architectures. All MOFs are topologically built upon secondary building units (SBUs), which are geometrical entities composed of metal clusters and organic linkers, forming robust and extended structures^[72]. These SBUs are typically formed *in situ* during carefully designed reaction processes. As fundamental components, the coordination geometry, ligand angularity, and the metal clusters that form SBUs collectively define the crystal structure of MOFs. According to the classification proposed by Tranchemontagne *et al.*^[73], the coordination numbers of SBUs can range from 3 to 66, reflecting their immense structural diversity; some examples of SBUs are shown in Figure 2B. This structural diversity enables MOFs to be tailored for specific applications, as slight modifications to the SBUs or their spatial arrangements can significantly alter their properties^[74,75]. These adaptable features also contribute to the sensing capabilities of MOFs, further broadening their potential applications.

MOFs possess unique structural features that distinguish them from conventional photocatalysts such as metal oxides^[76], sulfides^[77], or nitrides^[78]. They offer modular and customizable frameworks, which enable precise control over pore size, topology, and functionality. For instance, tunable pore dimensions can

accommodate large molecules, while adjustable bandgaps improve light absorption efficiency^[79]. Additionally, MOFs exhibit extraordinarily high surface areas and porosity, which enhance mass transport and reactant adsorption^[80]. The crystalline and periodic nature of MOFs ensures uniformity and consistency across active sites, a feature often lacking in amorphous or non-uniform compounds. Moreover, organic linkers in MOFs provide remarkable functional diversity, allowing for specific reactant interactions, enhanced electronic properties, and improved charge separation^[81]. These structural features form a foundation for further modifications to enhance photocatalytic performance.

Structural modification strategies for MOFs span multiple scales, enabling precise optimization for photocatalytic applications^[82,83]. At the macroscale and mesoscale levels, controlling particle size, morphology, and porosity is crucial for enhancing mass transport and reactant accessibility. Techniques such as templating or microwave-assisted synthesis enable the fabrication of hierarchical frameworks, including hollow spheres^[84] and nanosheets^[85], which improve diffusion efficiency and photocatalytic activity. The incorporation of MOFs into composite systems, such as metal oxides or carbon-based architectures, also creates synergistic effects that enhance light absorption and charge separation. At the atomic and electronic levels, modifications to metal nodes or functionalization of organic linkers allow fine-tuning of the electronic structure. These structural regulation strategies not only improve intrinsic photocatalytic properties but also expand the applicability of MOFs in energy conversion and environmental remediation.

The development of MOF structure regulation strategies

Leveraging their high surface area and tunable pore sizes, MOFs were initially applied in gas storage and separation^[86]. These early applications established a strong theoretical and practical foundation for the broader utilization of MOFs in energy and environmental fields^[87]. The photocatalytic potential of MOFs was first demonstrated by Alvaro *et al.*^[55], who revealed their capability in light-driven chemical reactions. This breakthrough sparked extensive research into the use of MOFs as photocatalysts, taking advantage of their unique structural features, such as tunable bandgaps and high porosity, for applications in water splitting^[88], CO₂ reduction^[89], and organic pollutant degradation^[90]. These investigations have positioned MOFs as versatile platforms to address critical challenges in sustainable energy production and environmental remediation.

As illustrated in Figure 3A, influential journals such as Chemical Engineering Journal and Applied Catalysis B: Environmental and Energy have significantly advanced research on MOF-based photocatalysts, emphasizing the importance of structural regulation in their design. Figure 3B highlights the exponential growth in publications on MOF photocatalysis since their initial use as photocatalysts to the present, underscoring the increasing focus on structural innovation. This trend reflects the pivotal role of tailoring MOF structures, including the optimization of metal nodes, organic linkers, and pore environments, to enhance photocatalytic efficiency. Collectively, these efforts demonstrate the continuous pursuit of novel MOF designs to address pressing energy and environmental challenges.

Since their initial application in photocatalysis, structural regulation strategies for MOFs have evolved rapidly, particularly after 2011. As shown in Figure 4, early breakthroughs included the development of MOF derivatives^[91], core-shell structures^[92], preparation of films^[93] and the encapsulation of guest molecules^[94], which significantly improved structural tunability and photocatalytic performance. With advancements in technology and deeper insights from research, recent milestones have shifted toward atomic-scale and electronic-scale modifications. These advancements encompass studies on functionalized ligands^[95], encapsulation with single atom^[96], orbital electrons^[97], crystal facet engineering^[98], charge transfer

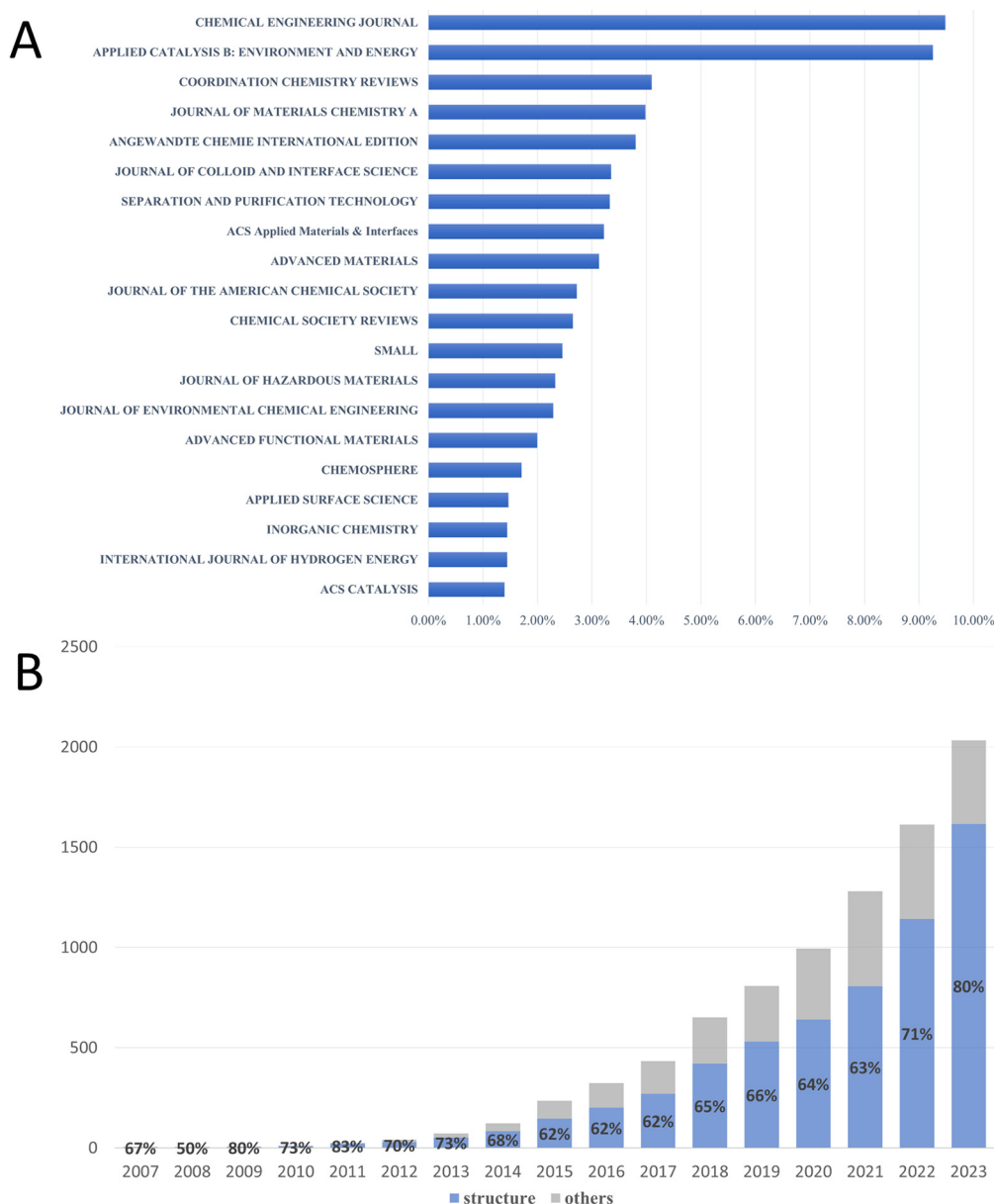


Figure 3. (A) Contribution from top 20 journals; (B) Annual publication trends and percentage changes in MOF structure-related research.

mechanisms^[99], and band bending^[100], which highlight the increasing complexity and precision of MOF research. These developments not only enhance the intrinsic properties of MOFs but also expand their applicability across diverse photocatalytic processes, reinforcing their transformative potential in sustainable technologies.

REGULATION OF MACROSCALE AND MESOSCALE STRUCTURES

Macroscale regulation

Macroscale regulation of MOFs focuses on enhancing their practical use and photocatalytic efficiency through various structural designs. Particle-based and film-based MOFs offer distinct advantages and drawbacks. Particle-based MOFs, with their high surface area, provide more active sites and efficient

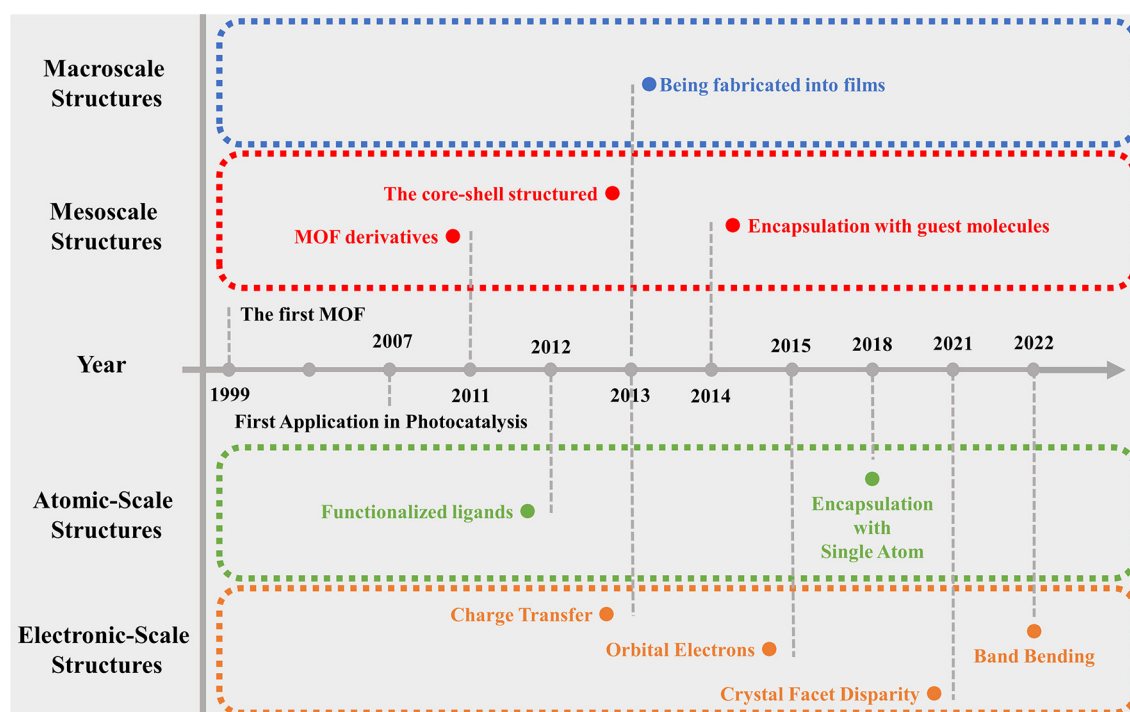


Figure 4. The development of MOFs as photocatalysts.

photocatalytic performance in suspension systems. However, issues such as difficult recovery and limited reusability restrict their broader use. In contrast, film-based MOFs offer excellent mechanical stability and are suitable for device integration, but their lower surface area and fabrication challenges reduce their overall effectiveness. This section reviews recent advancements in macroscale regulation, emphasizing strategies that leverage the unique characteristics of both particle- and film-based MOFs in photocatalysis.

Powders

Most MOFs are synthesized as powders, making particles the dominant morphology. This particle form offers several benefits for photocatalysis. MOF particles, with their high surface area and well-defined pores, provide abundant active sites and enhance interactions between reactants and photocatalysts. Their discrete morphology ensures excellent dispersibility in suspension systems, promoting uniform photocatalytic activity. Additionally, their solid-state form ensures stability in both aqueous and organic environments. Thus, controlling particle size and shape is crucial for optimizing photocatalytic performance.

Wang *et al.* explored the photocatalytic performance of Bi_2O_3 enhanced through the construction of $\text{Bi}_2\text{O}_3/\text{Cu-MOF}$ heterostructures, emphasizing the benefits of particle size reduction and structural optimization^[101]. Using a microwave-assisted method, $\text{Bi}_2\text{O}_3/\text{Cu-MOF}$ composites were synthesized, achieving efficient integration of Cu-MOF into the Bi_2O_3 framework. As illustrated in Figure 5A, the incorporation of Cu-MOF significantly reduced the particle size of Bi_2O_3 , resulting in smaller and more uniform particles compared to pristine Bi_2O_3 . This structural modification increased the specific surface area and improved the pore structure, thereby enhancing visible light utilization and charge transfer efficiency, ultimately achieving superior photocatalytic degradation of 1,4-dioxane.

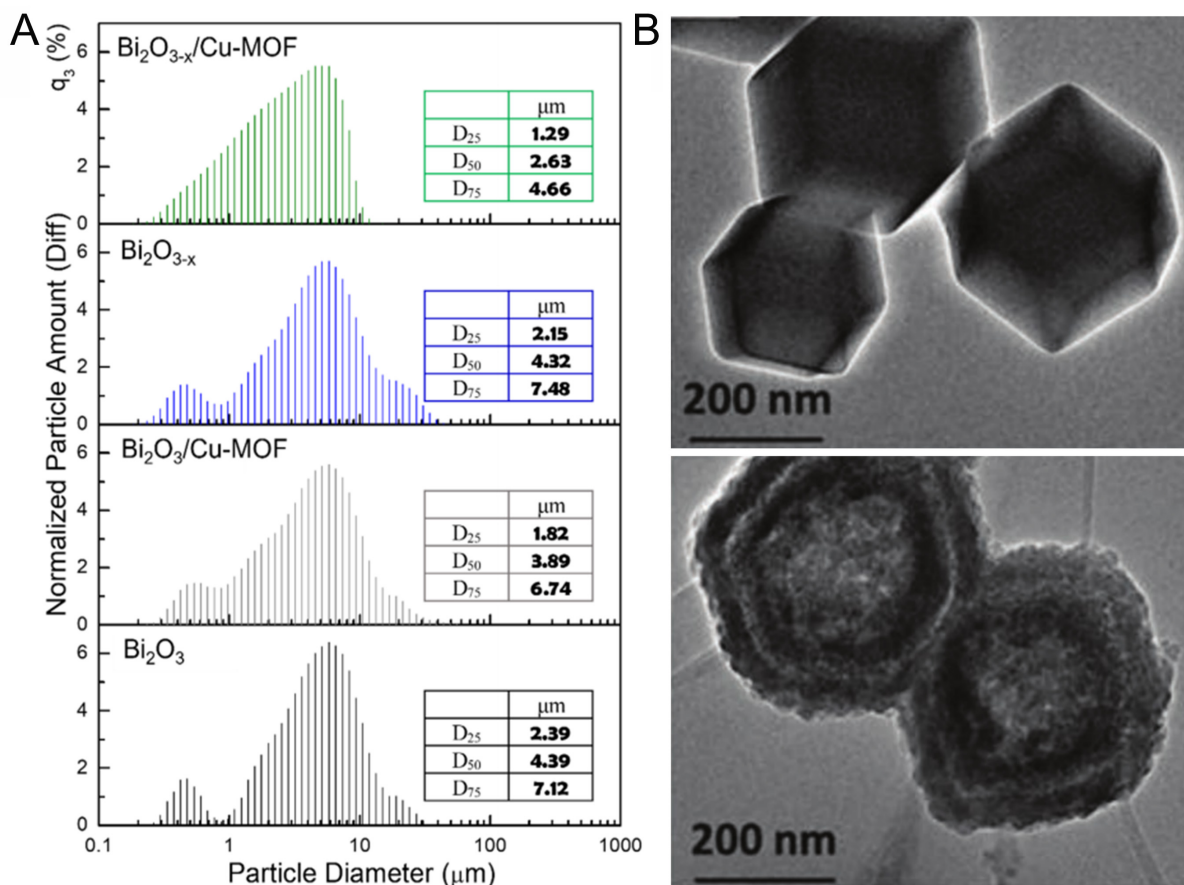


Figure 5. (A) Particle size distribution of Bi₂O₃/Bi₂O_{3-x}/Cu-MOF, Bi₂O_{3-x}, and Bi₂O_{3-x}/Cu-MOF; (B) SEM images of ZIF-67 and MOF-74-T. Reproduced with permission Ref.^[102] Copyright 2019 John Wiley and Sons.

Deng *et al.* demonstrated the benefits of constructing hollow Co-MOF-74 structures through a solvothermal transformation strategy^[102]. This method converted ZIF-67 into Co-MOF-74 with a double-layer hollow shell structure [Figure 5B], maintaining the original particle shape while increasing active site exposure and facilitating charge transfer. This structural advantage resulted in the photocatalytic activity of hollow Co-MOF-74 being 1.8 times higher than that of conventionally synthesized Co-MOF-74. Furthermore, composites of Ag nanoparticles@Co-MOF-74 achieved an impressive 3.8-fold increase in activity.

Films

MOF films for photocatalysis are typically prepared using methods such as layer-by-layer deposition, solvothermal growth, or spin coating, depending on desired properties such as thickness, crystallinity, and surface area. MOF films offer advantages over particle forms in certain applications. Their fixed structure provides better mechanical stability and reusability, making them ideal for integrated photocatalytic devices. Additionally, MOF films prevent issues such as particle aggregation, ensuring controlled exposure of active sites, which enhances their performance in continuous-flow systems and device fabrication.

In one study, Meng *et al.* developed a carbon fiber cloth (CFC)-based TiO₂/Ti-MOF nanorod array through a hydrothermal-solvothermal two-step process^[103]. As illustrated in Figure 6A, the membrane was grown directly on CFC, integrating the enhanced light absorption of TiO₂ with the photocatalytic properties of NH₂-MIL-125(Ti). This innovative design achieved a super-hydrophilic surface and light-trapping effects,

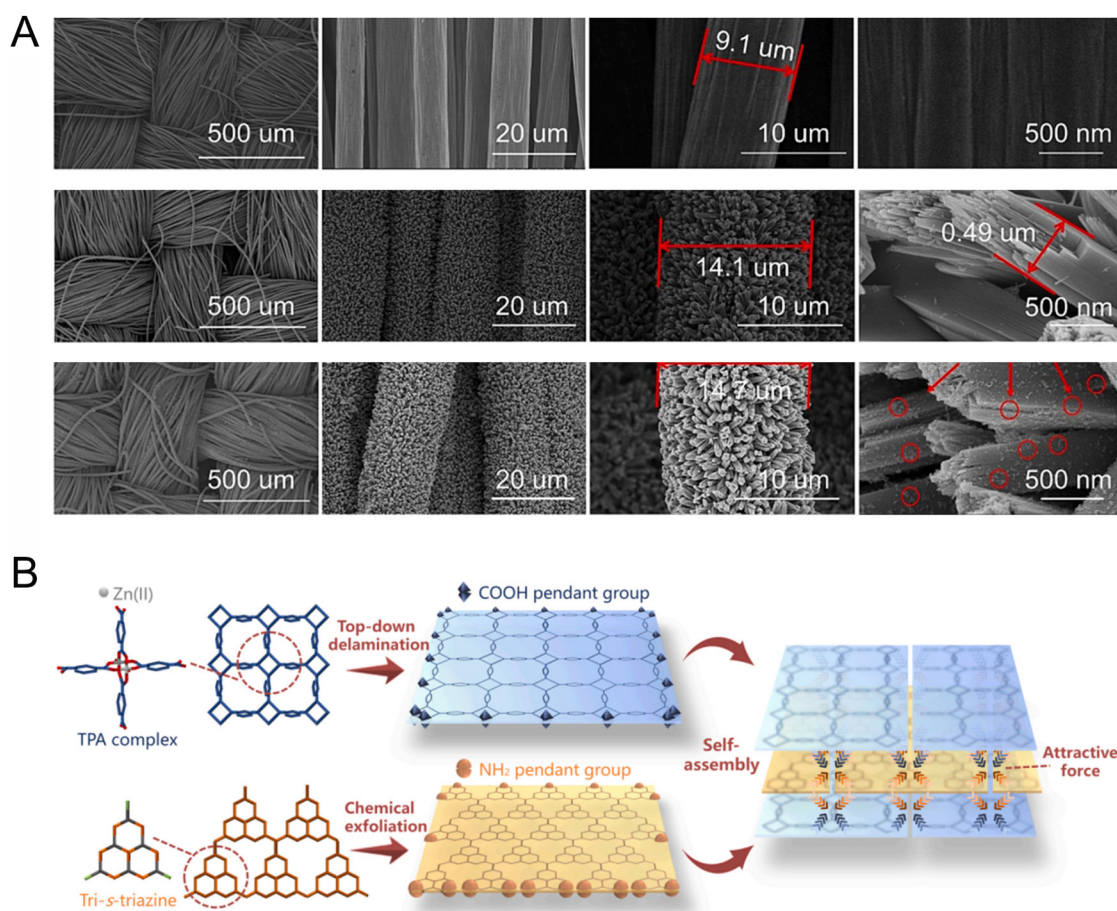


Figure 6. (A) SEM images of the CFc, CFc/TiO₂ and CFc/TiO₂/Ti-MOF. Reproduced with permission Ref.^[103] Copyright 2024 Elsevier. (B) (blue) forming the paddle-wheel secondary building units of MOF-2. Tertiary amino N (orange) and tri-s-triazine C (black) were conjugated in the heterocyclic rings of g-C₃N₄ in addition to the marginal N (green). Reproduced with permission Ref.^[104] Copyright 2022 Elsevier.

leading to superior removal efficiencies for organic pollutants and an evaporation rate of 1.86 kg·m⁻²·h⁻¹ without salt precipitation.

Similarly, Wang *et al.* explored a vacuum-assisted self-assembly process to fabricate a photocatalytic MOF membrane with a two-dimensional (2D) heterostructure^[104]. As shown in Figure 6B, the membrane was composed of alternately arranged ultrathin MOF-2 and g-C₃N₄ nanosheets, forming orderly interlayer nanochannels that broadened the light-harvesting range and suppressed charge carrier recombination. This novel structure also enforced fluid confinement and steric-hindrance effects, achieving a high permeation flux of 23.6 L·m⁻²·h⁻¹·bar⁻¹ and removal rates exceeding 89% for various pollutants.

Mesoscale regulation

MOFs typically range from nanometers to micrometers in size, placing them in the mesoscale domain. At this scale, strategies such as morphology control, pore size regulation, and MOF-based composites have been developed to optimize their properties for specific applications. Additionally, MOF derivatives, including carbon-based structures and metal oxides, can be synthesized through thermal or chemical processes. The incorporation of functional guest molecules further enhances tunability, enabling innovative mesoscale designs. These approaches are crucial for achieving precise control over MOF structure and

functionality, advancing their potential in photocatalysis and other applications.

Controllable fabrication of morphology

MOFs, with their tunable photocatalytic properties, exhibit diverse morphologies at the mesoscale, including 1D, 2D, and 3D structures, influenced by synthesis conditions and the properties of metal nodes and organic linkers. Each morphology offers distinct advantages: 1D structures, such as nanorods and nanowires, promote directional charge transport; 2D nanosheets optimize light absorption and active site exposure with large lateral dimensions and high surface-to-volume ratios; 3D architectures, such as hollow spheres and polyhedral crystals, combine high porosity and stability, enhancing mass transport and reactant diffusion. This morphological versatility makes MOFs ideal for customized photocatalytic applications across different scales and environments.

Gao *et al.* synthesized a rod-like 1D Bi-benzene-1,4-dicarboxylic acid (BDC) MOF photocatalyst using a microwave-assisted method, as depicted in [Figure 7A](#)^[105]. This 1D morphology offered a high surface area and efficient charge transport pathways, achieving complete Cr (VI) reduction within 6.0 min under low-power light-emitting diode (LED) ultraviolet (UV) light in the presence of tartaric acid (TA). Furthermore, the photocatalyst maintained stable performance over five consecutive cycles, demonstrating minimal sensitivity to environmental factors such as pH and inorganic ions. In another study, Liang *et al.* synthesized 2D monolayer and bilayer porphyrin-based MOFs by adjusting the reaction temperature and solvent polarity, as shown in [Figure 7B](#)^[106]. The bilayer MOF exhibited a distinctive dislocated structure, where the upper and lower layers were bridged by halogen ions, enhancing its photocatalytic properties. This 2D structure achieved 100% selectivity for CO reduction to CO under simulated sunlight without the need for a cocatalyst or photosensitizer, and it demonstrated stable recyclability over three cycles. Taking a different approach, Song *et al.* designed an S-scheme heterojunction to enhance CO₂ reduction activity in ZnIn₂S₄/MOF-808 microspheres via an *in-situ* synthesis method, as depicted in [Figure 7C](#)^[107]. The 3D heterojunction, comprising ZnIn₂S₄ microspheres coupled with octahedral MOF-808, achieved a CO yield of 8.21 $\mu\text{mol}\cdot\text{g}^{-1}\cdot\text{h}^{-1}$ - 10 and 8 times higher than pure ZnIn₂S₄ and MOF-808, respectively.

Pore size

The regulation of pore size is an important factor in improving the photocatalytic performance of MOFs. Hierarchical porosity, combining micro- and mesopores, enhances mass transport, reactant accessibility, and interactions with active sites. By reducing diffusion resistance and promoting charge separation, tuning pore size helps optimize MOF-based photocatalysts for environmental and energy applications.

Chen *et al.* synthesized MIL-100(Fe) MOF/MOF xerogels (MOX) with tunable hierarchical pores using a one-pot solvothermal method^[108]. As shown in the SEM images of different pore-sized MOX in [Figure 8A](#) and their pore size distribution in [Figure 8B](#), the hierarchical pores were achieved by adjusting the anion species in the metal precursors to control the dissociation rate of metal ions. This process created both micro- and mesopores (2-10 nm), reducing diffusion resistance and enabling effective contact between gaseous BTXS (benzene, toluene, xylenes, and styrene) molecules and active sites. The resulting material demonstrated significantly enhanced photocatalytic oxidation performance, highlighting the critical role of pore size regulation in improving efficiency for gaseous pollutant removal.

MOF-based hybrids

MOF-based hybrids enhance photocatalytic performance by integrating complementary photocatalysts. These hybrids combine the high surface area and tunable porosity of MOFs with improved charge separation and broader light absorption. Examples include MOF-semiconductor hybrids, MOF-carbon

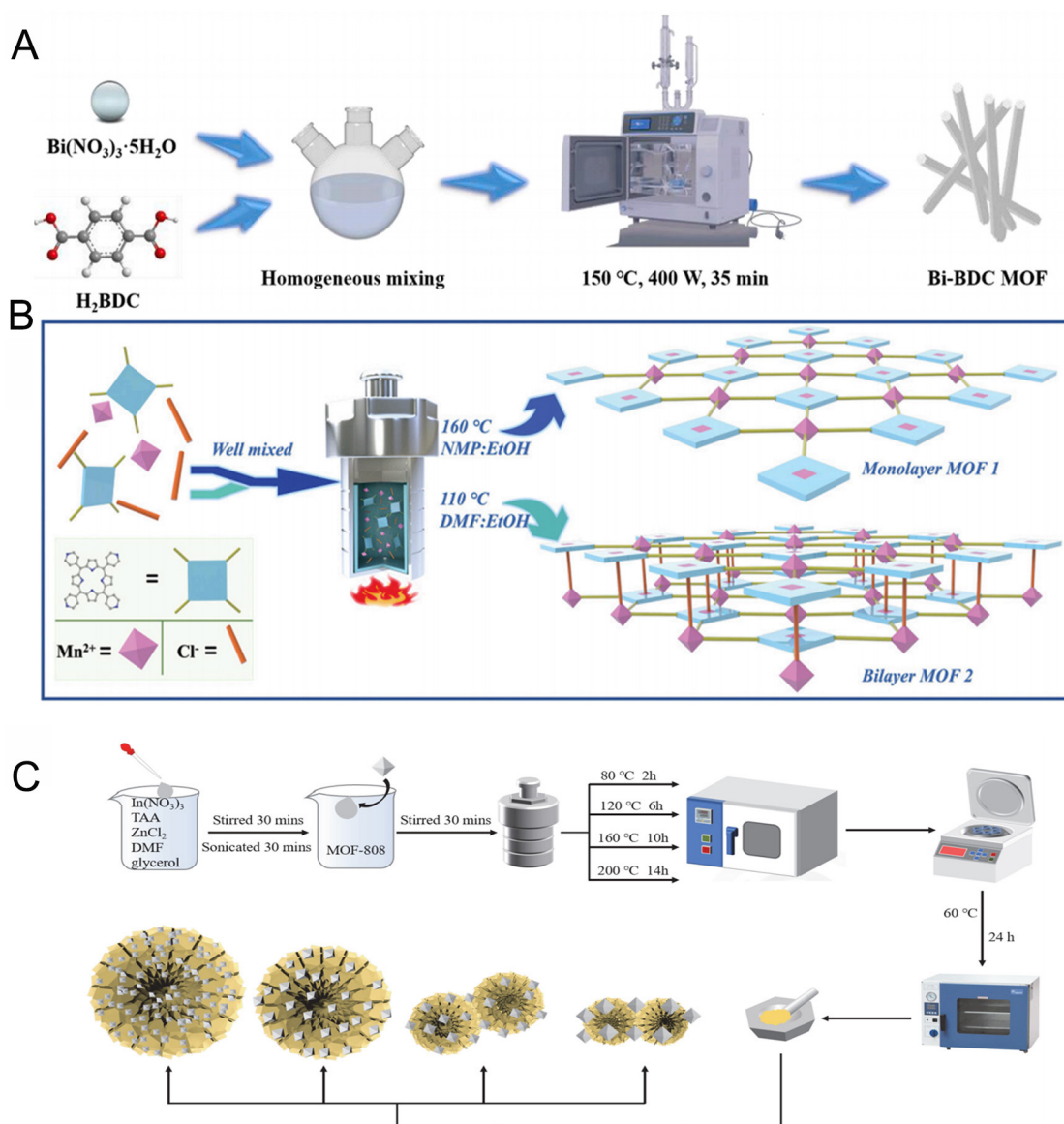


Figure 7. (A) The illustration of Bi-BDC MOF fabrication by microwave-assisted method. Reproduced with permission Ref. [105] Copyright 2023 Elsevier. (B) Preparation Process of Monolayer and Bilayer MOFs. Reproduced with permission Ref. [106] Copyright 2023 John Wiley and Sons. (C) Preparation process of $\text{ZnIn}_2\text{S}_4/\text{MOF-808}$. Reproduced with permission Ref. [107] Copyright 2023 Elsevier.

hybrids, MOF-nanoparticle hybrids, and MOF-organic frameworks. Each type boosts photocatalytic efficiency through mechanisms such as enhanced charge transfer, wider light absorption, or better active site accessibility. This section focuses on MOF-MOF hybrids, MOF-COF hybrids and MOF-nanoparticle hybrids, which show synergies and structural features that benefit photocatalytic applications.

MOF-MOF hybrids combine the distinct properties of different MOFs, creating synergies that enhance photocatalytic performance. For example, Yuan *et al.* constructed a Step-scheme (S-scheme) MIL-125- NH_2 @CoFe Prussian blue analog (PBA) MOF-on-MOF heterojunction using a selective assembly method, as illustrated in Figure 9A [109]. This heterostructure featured a hollow sandwich-like morphology, where CoFe PBA nanocages were selectively assembled on the surfaces of MIL-125- NH_2 nanocakes. Interfacial Ti-O-Co bonds at the junction generated an internal electric field, accelerating charge transfer

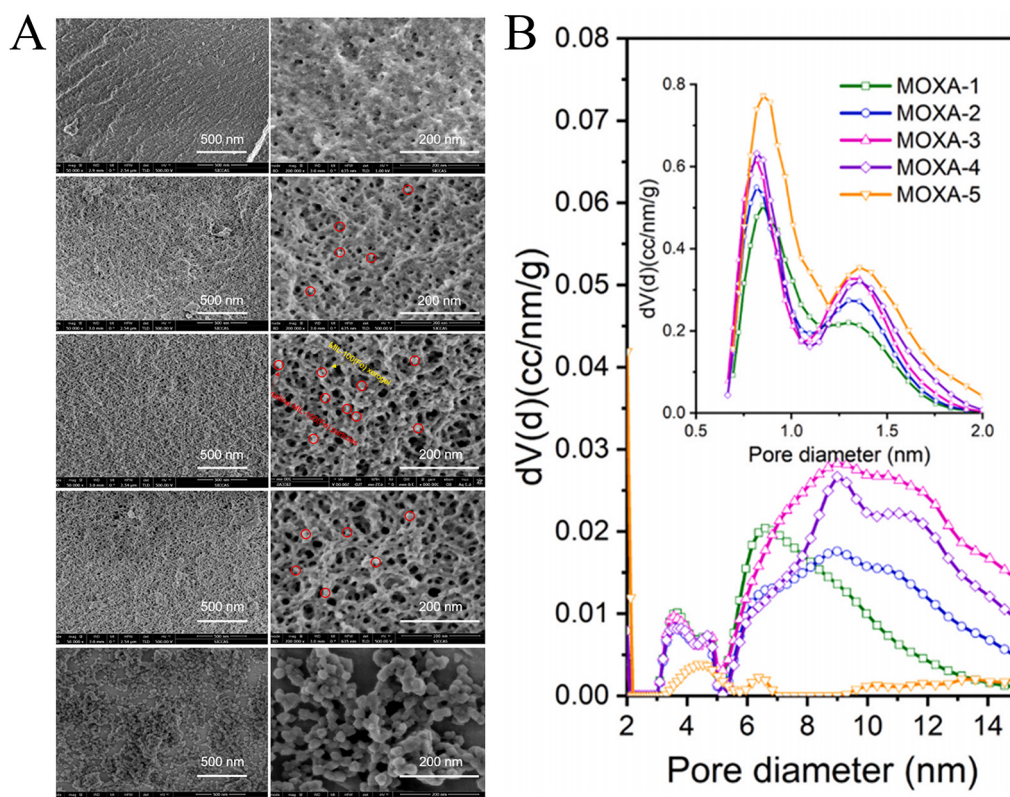


Figure 8. (A) SEM images of MOXA-1, MOXA-2, MOXA-3, MOXA-4, and MOXA-5; (B) pore size distributions of MOXA-1, MOXA-2, MOXA-3, MOXA-4, and MOXA-5. Reproduced with permission Ref. [108] Copyright 2022 Elsevier.

and improving redox performance. This design significantly enhanced the photocatalytic degradation of organic pollutants, showcasing the potential of MOF-MOF heterojunctions.

MOF-COF hybrids merge the properties of MOFs and COFs, achieving enhanced photocatalytic performance by improving charge transfer and stability. Li *et al.* developed hierarchical MOF/COF hybrids via a post-synthetic covalent modification strategy, bonding benzoic acid-modified covalent triazine-based framework (CTF)-1 with MOFs such as NH_2 -MIL-125(Ti) [110]. Schematic illustration of the formation of NH_2 -MIL-125(Ti)/B-CTF-1 (TBC) hybrid material is shown in Figure 9B. These hybrids demonstrated enhanced photocatalytic hydrogen production under visible light, attributed to improved charge separation and photocatalyst stability.

Qin *et al.* fabricated a $ZnO/Uio66-NH_2$ heterojunction using a partial calcination strategy, encapsulating ultra-small ZnO particles within the porous $Uio66-NH_2$ framework while preserving the MOF's structural integrity [111]. The preparation route, structure, and morphology of photocatalysts are shown in Figure 10. This encapsulation ensured MOF stability while facilitating enhanced charge and mass transfer, creating an efficient channel for photocatalytic reactions. The $ZnO/Uio66-NH_2$ composite demonstrated high activity in converting polylactic acid (PLA) and polyvinyl chloride (PVC) into acetic acid, alongside concurrent H_2 production.

MOF-based derivatives

MOF-based derivatives are advanced photocatalysts created through thermal, chemical, or structural

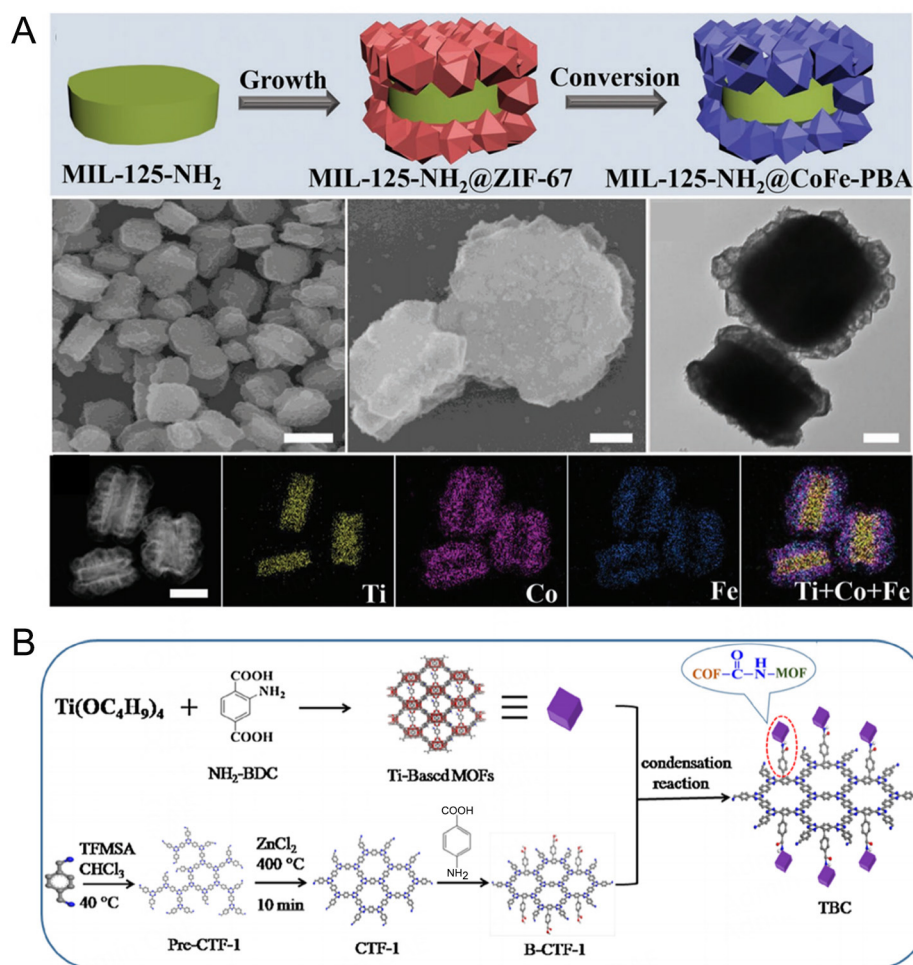


Figure 9. (A) Illustration of the synthesis process of MIL-125-NH₂@CoFe PBA, SEM, TEM, HAADF-STEM and corresponding element mapping images. Reproduced with permission Ref.^[109] Copyright 2023 John Wiley and Sons. (B) Schematic illustration of the formation of TBC hybrid material. Reproduced with permission Ref.^[110] Copyright 2019 Elsevier.

transformations of MOFs, retaining their porous structure while introducing new functionalities. These derivatives, including metal oxides, sulfides, carbon, and hybrid composites, combine the structural benefits of MOFs with enhanced photocatalytic properties. By maintaining high porosity and well-distributed active sites, they ensure efficient mass transport and reactant accessibility. Additionally, the transformation process improves thermal stability, electrical conductivity, and active site density. This makes MOF-based derivatives a versatile platform for designing next-generation photocatalysts, expanding their use in energy conversion and environmental remediation^[112]. Among these derivatives, MOF-derived oxides and sulfides have gained significant attention due to their enhanced properties and diverse applications. These derivatives, obtained through controlled thermal or chemical transformations of MOFs, exhibit remarkable improvements in several key photocatalytic characteristics, including enhanced charge carrier mobility, stability, and active site density^[113].

MOF-derived oxides, such as cobalt oxide, iron oxide, and titanium oxide, are widely used in photocatalysis due to their high stability and excellent electron transfer properties. On the other hand, MOF-derived sulfides, such as ZnS and CdS, are also gaining attention due to their ability to effectively utilize visible light in photocatalytic reactions. For instance, Ren *et al.* developed a dual cobalt active species encapsulated

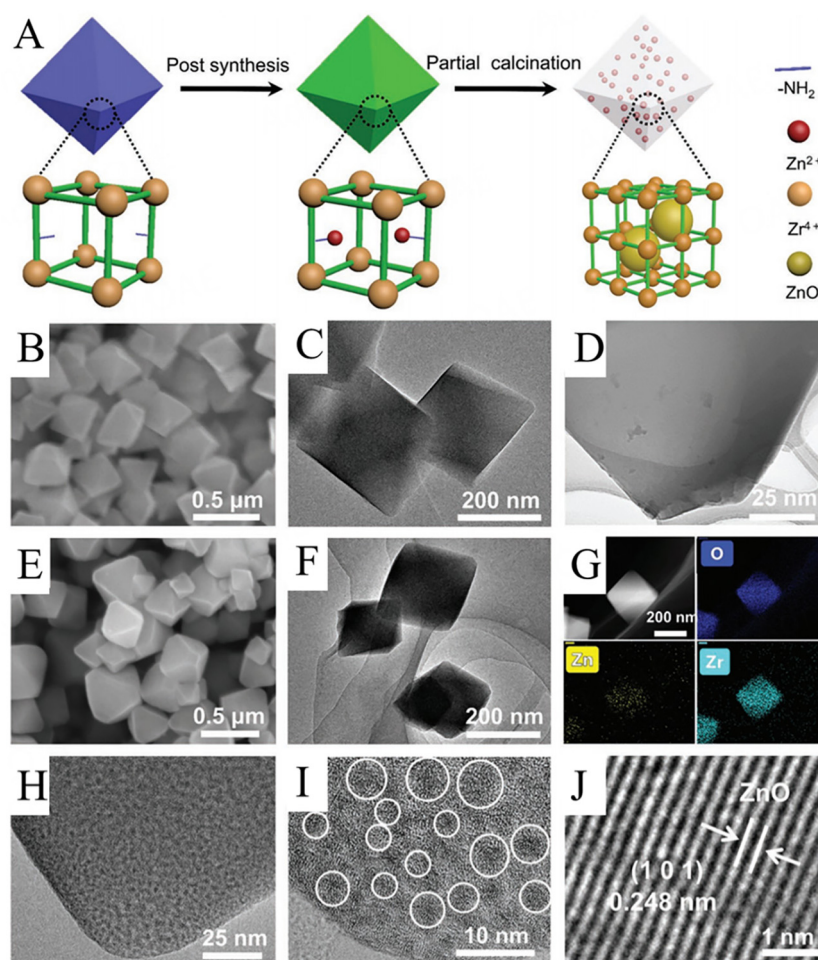


Figure 10. Preparation route, structure, and morphology of photocatalysts. (A) Schematic illustration of the fabrication of ZnO/UiO66-NH₂ via post-synthesis and subsequent partial calcination; (B-D) SEM image and low-magnification TEM images of UiO66-NH₂, respectively; (E-G) SEM image, low-magnification TEM image and EDX mapping of ZnO/UiO66-NH₂, respectively; (H-J) TEM images of ZnO/UiO66-NH₂. Reproduced with permission Ref. [111] Copyright 2023 John Wiley and Sons.

within an ultrathin carbon matrix derived from 2D Co-MOF nanosheets^[114]. As illustrated in Figure 11, the assembly and pyrolysis process produced Co and CoOx species embedded in the carbon matrix, spatially separated to optimize charge extraction and minimize recombination. This structural refinement enhanced charge carrier mobility and photogenerated electron-hole separation, resulting in improved photocatalytic H₂ evolution under visible light. The derived material, CdS-Co-CoOx@C, exhibited a 12.5-fold increase in H₂ production compared to pristine CdS, with an apparent quantum efficiency of 43.7% at 420 nm. Liang *et al.* synthesized 1D spindle-like iron oxides (Fe₃O₄ and α -Fe₂O₃) using MIL-88A as a sacrificial template through pyrolysis and constructed 2D/1D core-shell heterostructures (ZnIn₂S₄@Fe₃O₄ and ZnIn₂S₄@ α -Fe₂O₃) via an *in-situ* self-assembly strategy^[115]. Among these, the ZnIn₂S₄@Fe₃O₄ composite demonstrated a higher Brunauer-Emmett-Teller (BET) surface area of 84.5 m² g⁻¹ compared to ZnIn₂S₄@ α -Fe₂O₃, providing more active sites and improving photocatalytic degradation efficiency for pollutants such as rhodamine B (RhB), methylene blue (MB), bisphenol A (BPA), and methyl orange (MO). The Fe³⁺/Fe²⁺ redox cycle in Fe₃O₄ facilitated a Z-scheme charge transfer pathway, which contributed to the enhanced photocatalytic activity observed in this composite.

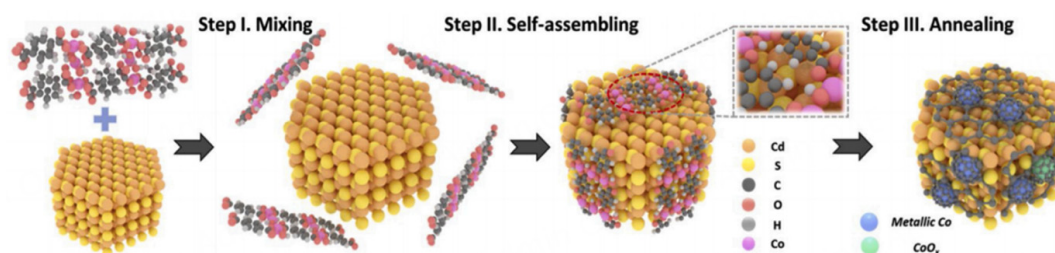


Figure 11. Schematically illustration of preparing CdS-Co-CoO_x@C from self-assembly CdS-Co-MOF precursor. *In-situ* FTIR spectra measured. Reproduced with permission Ref.^[114] Copyright 2021 Elsevier.

Both MOF-derived oxides and sulfides offer unique advantages in photocatalysis, including tunable properties through the control of their synthesis processes. The high surface area and porosity retained from the parent MOF structures allow for improved interaction with reactants, while the transformation into oxides or sulfides introduces new active sites and better charge separation, leading to enhanced photocatalytic efficiencies.

REGULATION OF ATOMIC-SCALE AND ELECTRONIC-SCALE STRUCTURES

Atomic-scale regulation

Atomic regulation in MOFs involves adjusting the coordination environment of metal ions, functionalizing organic linkers, and modifying crystal structures to optimize photocatalytic performance. These atomic-scale adjustments improve active site accessibility, structural stability, and adaptability for various photocatalytic applications. By addressing challenges in efficiency and selectivity, these strategies enable precise tuning of MOF properties. This section explores key atomic regulation methods and their impact on MOF properties and applications.

Metal ions

Metal ions in MOFs play a crucial role in their structural integrity and photocatalytic efficiency, serving as active sites that influence stability and reactivity. Transition metals such as Ti, Zr, and Fe enhance structural stability and photocatalytic performance, while rare-earth metals provide electronic configurations ideal for selective reactions. Table 1 summarizes various metal ions used in photocatalysis. The choice of metal ions affects the photocatalytic performance and should match the specific needs of the photocatalytic process.

Zhang *et al.* synthesized a mixed-valence Fe(II/III) MOF (BIT-108) by partially oxidizing Fe(II) ions in Fe(II)₂N₂O₁₀ clusters using a solvent displacement method^[135]. The mixed valence states, combined with O, N co-coordination in the iron clusters, optimized the electronic band structure and improved charge transfer dynamics. This adjustment led to a 25-fold increase in H₂ evolution under visible-light irradiation compared to the parent Fe(II) MOF. Furthermore, BIT-108 outperformed traditional photocatalysts such as α -Fe₂O₃ and NH₂-UiO-66, showcasing the advantages of manipulating the valence states and coordination environment of metal ions.

Functionalized ligands

In MOFs, organic linkers or ligands connect metal nodes and influence the framework's structure, stability, and functionality. Ligands affect electronic properties, pore size, and surface functionality. Functionalizing ligands with specific chemical groups can enhance light absorption, improve charge transfer, or increase interaction with target molecules^[136]. For example, adding electron-rich or electron-withdrawing groups can adjust electronic properties, improving photocatalytic performance, stability, or selective interactions with

Table 1. Applications of MOFs with different metal ions

Metal ion type	Photocatalyst	Application	Ref.
Ag	Ag-MOF in polyvinyl alcohol films	Antimicrobial packaging films	[116]
Al	Al-MOF with porphyrin and pyrene linkers	Photosynthesis of H ₂ O ₂	[117]
Bi	Bi-MOF	Degradation of organic pollutant	[118]
Ca	Triphenylamine-based Ca-MOF	Promoting photocatalysis	[119]
Ce	Ce-MOF modified ceria-based photocatalyst	Degradation of organic pollutants	[120]
Co	Co-MOF with Bi ₂ MoO ₆	CO ₂ reduction t	[121]
Cr	Cr-MOF	Interfacial solar-driven steam generation	[122]
Cu	Ag ₃ VO ₄ /Cu-MOF/rGO	Degradation of organic pollutants	[123]
Gd	Gd-MOF with azo-carboxylic acid	Hydrogen evolution	[124]
La	UiO-66/La-MOF composite with H ₂ BDC and H ₂ ATA	Degradation of dyes	[125]
Mg	MgO nanorods derived from Mg-MOF	Decolorization of methylene blue	[126]
Mn	Ni/Mn-MOF	Photocatalysis and energy storage	[127]
Nd	Nd-MOF/GO/Fe ₃ O ₄	Dye degradation	[128]
Ni	ZnFe ₂ O ₄ @Co/Ni-MOF	Degradation of azo dyes	[129]
Pd	Pd-TCPP based 2D MOF nanosheets	Hydrogen evolution	[130]
Pt	Pt-MOF with Au deposition	Hydrogen evolution	[131]
Sn	Sn-MOF and Sn-MOF@Fe ₃ O ₄ composites	Degradation of rhodamine B	[132]
Zn	Zn-MOF	Sensing of L-tryptophan and degradation of tetracycline	[133]
Zr	Zr-MOF decorated with CdS through pore functionalization	Hydrogen evolution	[134]

rGO: Reduced graphene oxide; GO: graphene oxide; H₂BDC: terephthalic acid; H₂ATA: 2-amino terephthalic acid; TCPP: porphyrin.

substrates. This section explores ligand functionalization strategies and their role in optimizing MOF photocatalytic properties for various applications.

Mao *et al.* developed UiO-66-Cu-CdS/ZnS (SCu-CZS), by loading CdS/ZnS quantum dots onto thiol-functionalized UiO-66 (UiO-66-SH) through a straightforward synthesis method, as depicted in Figure 12A^[137]. The incorporation of thiol-functionalized ligands facilitated efficient charge separation and transfer between CdS and ZnS quantum dots. This ligand modification enhanced the charge transfer mechanism, significantly improving photocatalytic hydrogen evolution performance. The optimized SCu-CZS achieved a hydrogen generation rate of 425.5 μmol/h without requiring noble metal cocatalysts, demonstrating the potential of ligand functionalization for improving charge dynamics in MOFs.

Zhang *et al.* applied an organic ligand regulation strategy to synthesize four novel Fe-MOFs for enhanced photocatalytic Cr (VI) reduction, with the synthesis process and structures illustrated in Figure 12B^[138]. By introducing -SCH₃ functional groups and TPT ligands, they improved light absorption and spatial separation of photogenerated charge carriers through an enhanced electron push-pull effect. Among the synthesized MOFs, MTBDC-TPT-Fe exhibited the highest photocatalytic activity, efficiently reducing Cr (VI) without the need for sacrificial agents.

Grape *et al.* synthesized SU-101, the first bioinspired microporous MOF, using ellagic acid - a natural antioxidant and polyphenol - as the linker under ambient aqueous conditions, as shown in Figure 12C^[139]. This MOF, constructed with Bi³⁺ cations and ellagic acid, exhibited exceptional chemical stability and biocompatibility. The phenolic functional groups in ellagic acid strongly chelated Bi³⁺, contributing to the MOF's resistance to harsh environments, including acidic and basic pH, hydrothermal conditions, and exposure to organic solvents.

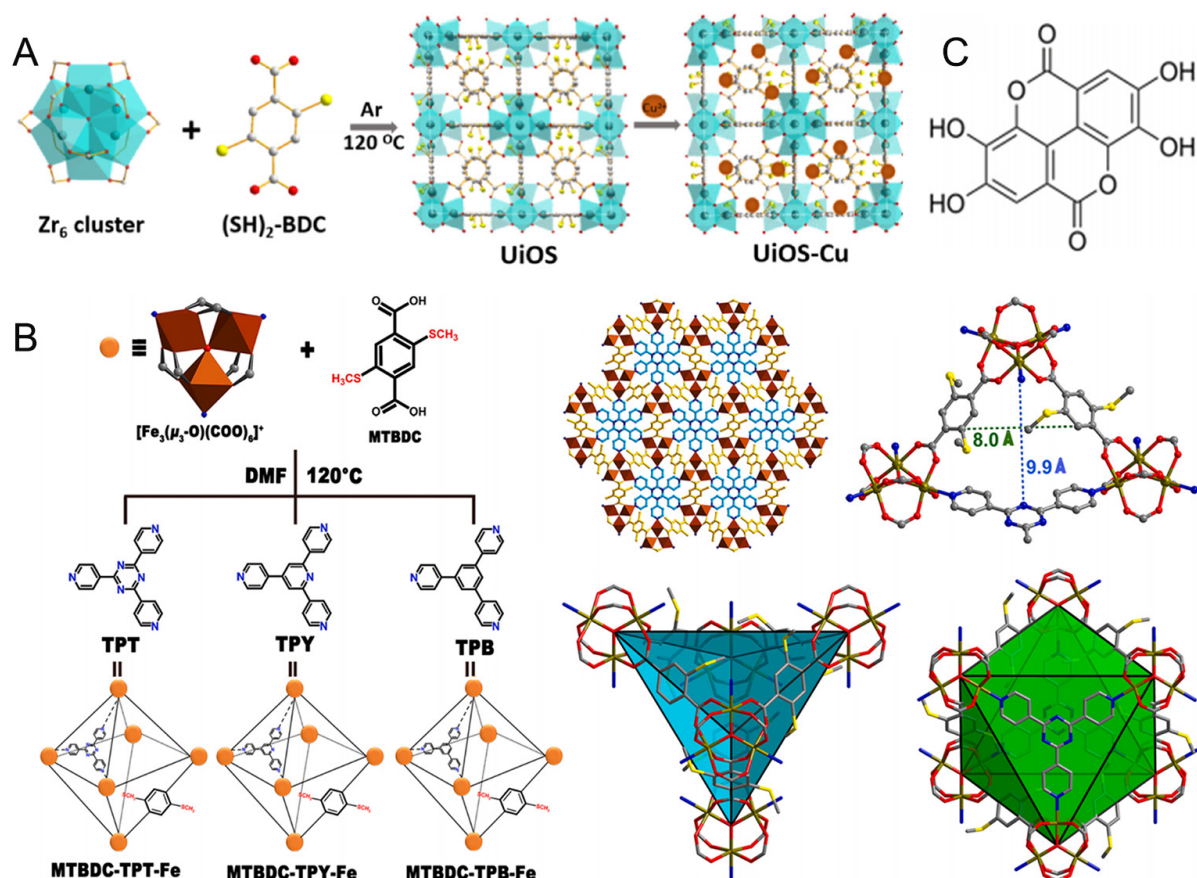


Figure 12. (A) Schematic illustration of the synthesis process of UiOS-Cu composite. Reproduced with permission Ref. [137] Copyright 2021 Elsevier. (B) Synthesis scheme of Fe-MOFs in this work, view of the 3D structure of MTBDC-TPT-Fe along the c axis, the window size of MTBDC-TPT-Fe, the triangular biconical cage of MTBDC-TPT-Fe and the distorted octahedral cage of MTBDC-TPB-Fe. Reproduced with permission Ref. [138] Copyright 2023 Elsevier. (C) Ellagic acid.

Crystal structure

The crystal structure of MOFs is highly versatile, influenced by the wide variety of metal ions and organic ligands used in their synthesis. This flexibility results in diverse geometries, such as cubic, hexagonal, and trigonal structures, each optimized for specific applications. Variations in coordination geometry, metal-ligand bonding, and linker functionality lead to different crystal structures, which influence properties such as light absorption, charge transport, and active site accessibility. This diversity is advantageous for photocatalysis, as it allows MOFs to selectively interact with target molecules, enhancing photocatalytic efficiency. By utilizing the unique properties of MOF crystal structures, researchers can design tailored photocatalysts for advanced applications.

Song *et al.* synthesized two Ni-based MOFs with distinct crystal forms through a reaction of bulk $Ni(OH)_2$ and BDC in N,N -Dimethylformamide (DMF)- H_2O solvents, as depicted in Figure 13A [140]. The resulting Ni-MOF(H_2O) displayed a thicker plate morphology, lower Ni content, and a smaller BET surface area compared to Ni-MOF. Despite these differences, Ni-MOF(H_2O) demonstrated a 1.8-fold higher CO_2 yield in the photocatalytic reduction of CO_2 . This enhanced activity was attributed to stronger CO_2 adsorption, improved charge transfer, and a reduced recombination rate of photogenerated carriers. Zhang *et al.* developed a site-selective etching method for CAU-17 microrods using Te- and Se-containing oxyanions, leading to distinct morphological transformations, as illustrated in Figure 13B [141]. The $TeOx^{2-}$ -mediated

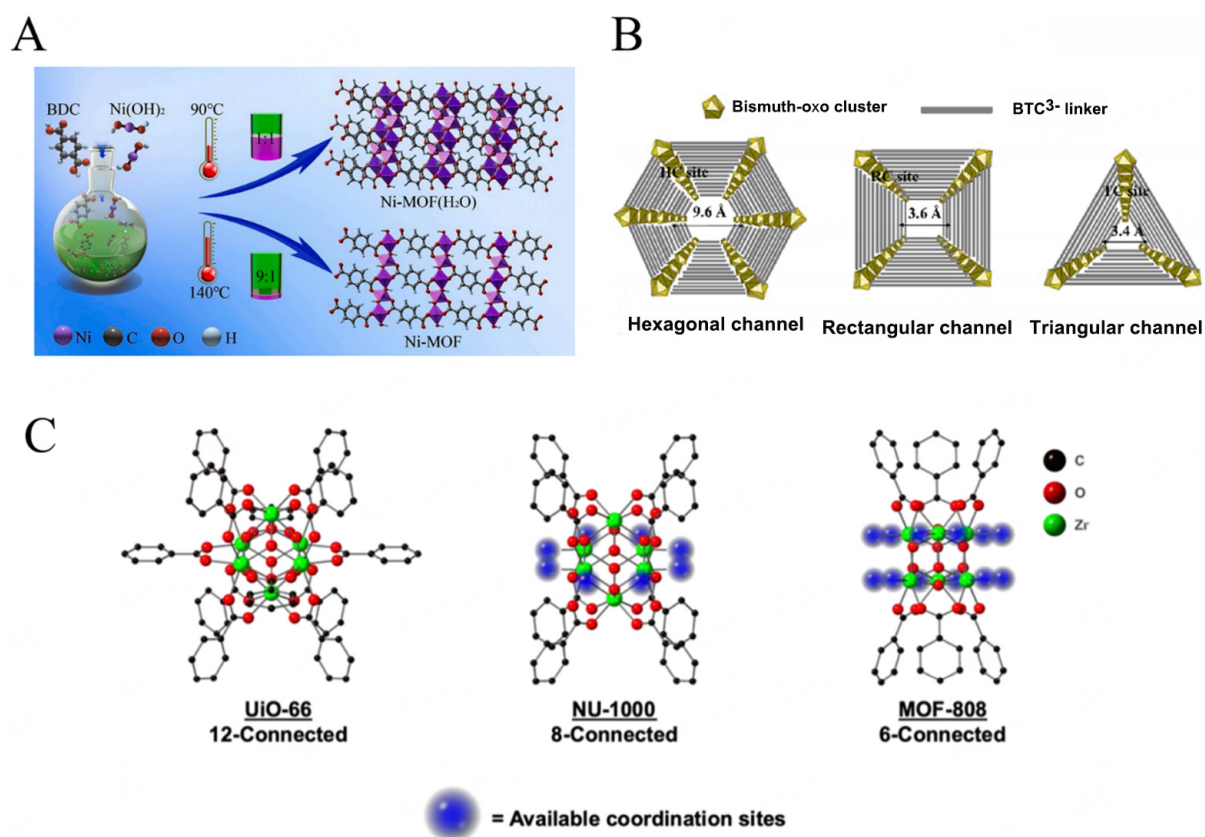


Figure 13. (A) Schematic illustration of the synthesis process of Ni-MOF (H₂O) and Ni-MOF. Reproduced with permission Ref. [140] Copyright 2022 Elsevier. (B) Structures of three types of channels in CAU-17. Reproduced with permission Ref. [141] Copyright 2024 Elsevier. (C) Examples of Zr-MOFs sharing the same Zr₆O₈ cluster but with varying connectivity. Reproduced with permission Ref. [142] 2022 Copyright American Chemical Society.

process yielded hollow tubular structures, while SeOx²⁻ induced sponge-like porous structures. These structural changes, facilitated by interactions with Bi-O bonds, enhanced the ability of MOFs to selectively and irreversibly capture radiotoxic oxyanions from wastewater. Hicks *et al.* investigated the influence of Zr-MOF topologies, including NU-1000, MOF-808, and UiO-66, on photocatalytic activity for 1-butene hydrogenation and isomerization, as shown in Figure 13C [142]. By applying thermal pre-treatments to modify Zr₆O₈ nodes, they demonstrated that the spatial arrangement of active sites significantly influences photocatalytic properties.

Electronic-scale regulation

MOFs are versatile photocatalysts, and electronic regulation is key to enhancing their performance. Similar to other photocatalysts, MOFs can be engineered to optimize their electronic structures, improving properties like charge carrier dynamics, light absorption, and photocatalytic efficiency. Electronic regulation strategies in MOFs include tuning the band structure, creating efficient charge transfer pathways, modulating electronic orbitals, and controlling electron spin. These approaches enable precise control over electronic properties, improving charge separation, electron transfer, and photocatalytic reactions. Fine-tuning MOF electronic structures helps overcome limitations such as slow charge carrier mobility and limited light absorption, which hinder traditional photocatalysts. For instance, bandgap engineering allows MOFs to absorb light in the visible spectrum, while orbital regulation enhances interaction with reactants.

Band structure

The electronic band structure of MOFs plays a key role in their photocatalytic properties, influencing light absorption, charge carrier dynamics, and photocatalytic activity. Tailoring the band structure optimizes energy alignment between the MOF and reactants, improving charge separation and reducing recombination. Methods such as adjusting metal coordination, functionalizing ligands, and doping can modify the CB and VB positions. These changes improve light absorption in specific regions and enhance the utilization of photogenerated electrons and holes, boosting photocatalytic performance.

In a study by Ding *et al.*, a Ru/MOF/C₃N₄ photocatalyst was synthesized by confining single Ru atoms within a MOF combined with graphitic carbon nitride (C₃N₄)^[143]. The resulting photocatalyst exhibited strong photocatalytic activity for carbon dioxide reduction reaction (CO₂RR) and nitrogen reduction reaction (NRR), tested under gas-solid and liquid-solid modes, respectively. The incorporation of Ru atoms introduced localized energy levels within the bandgap, reducing photogenerated carrier recombination and increasing carrier concentration. The changes in band structure following Ru doping are illustrated in Figure 14A. Furthermore, Ru atoms suppressed the hydrogen evolution reaction (HER) and lowered the Gibbs free energy for CO₂RR and NRR, contributing to improved photocatalytic performance. In another study, Li *et al.* synthesized Sn-doped MOF-5 (Sn-MOF-5) photocatalysts to improve nitrogen fixation performance^[144]. A series of Sn-MOF-5 photocatalysts were fabricated and tested using a T-tube photocatalysis reactor. Sn⁴⁺ doping increased the specific surface area and reduced capacity of MOF-5 while reducing its bandgap, facilitating better separation of photogenerated carriers. The band structure at different doping levels is shown in Figure 14B. Among these photocatalysts, Sn-MOF-5 with a Zn ratio of 6 achieved the highest photocatalytic performance, yielding 3,912.76 $\mu\text{mol}\cdot\text{L}^{-1}\cdot\text{g}^{-1}$ of ammonia (NH₃) after 5 h of photocatalysis, with stability maintained over 15 h of continuous operation.

Charge transfer

Charge transfer is a critical factor in the photocatalytic efficiency of MOFs, occurring through two main pathways: intraframe charge transfer within the MOF structure and interframe charge transfer between the MOF and external systems. While intraframe charge transfer has been discussed, this section focuses on interframe charge transfer, which involves interactions with cocatalysts, substrates, or surrounding media. Efficient interframe charge transfer establishes electron and hole migration pathways, improves charge carrier separation, reduces recombination rates, and enhances photocatalytic activity^[145]. By facilitating this process, MOFs can create synergistic systems that optimize both their structural and electronic properties for better photocatalytic performance.

Zhao *et al.* developed a 2D Zn-MOF/BiVO₄ S-scheme heterojunction (Zn-MOF/BVON) for efficient photocatalytic CO₂ conversion under visible light^[146]. As shown in Figure 15, the S-scheme charge transfer pathway improved charge separation and reduced recombination, significantly enhancing photocatalytic efficiency. The Zn-MOF/BVON heterojunction exhibited a 22-fold increase in photocatalytic activity compared to BiVO₄ nanoflakes and a twofold improvement over the g-C₃N₄/BiVO₄ heterojunction. This performance was attributed to the dimension-matched interface and well-dispersed Zn₂(COO)₄ metal nodes, which facilitated CO₂ activation. This study demonstrates the use of porphyrin-based MOFs in S-scheme heterojunctions for solar fuel production.

Electron orbitals

In MOFs, the interaction between metal-centered d-orbitals and ligand-based π -orbitals determines important electronic properties, such as bandgap and energy alignment. These electron orbitals facilitate photon absorption, exciting electrons from the VB to the CB, driving photocatalytic reactions. By tuning the

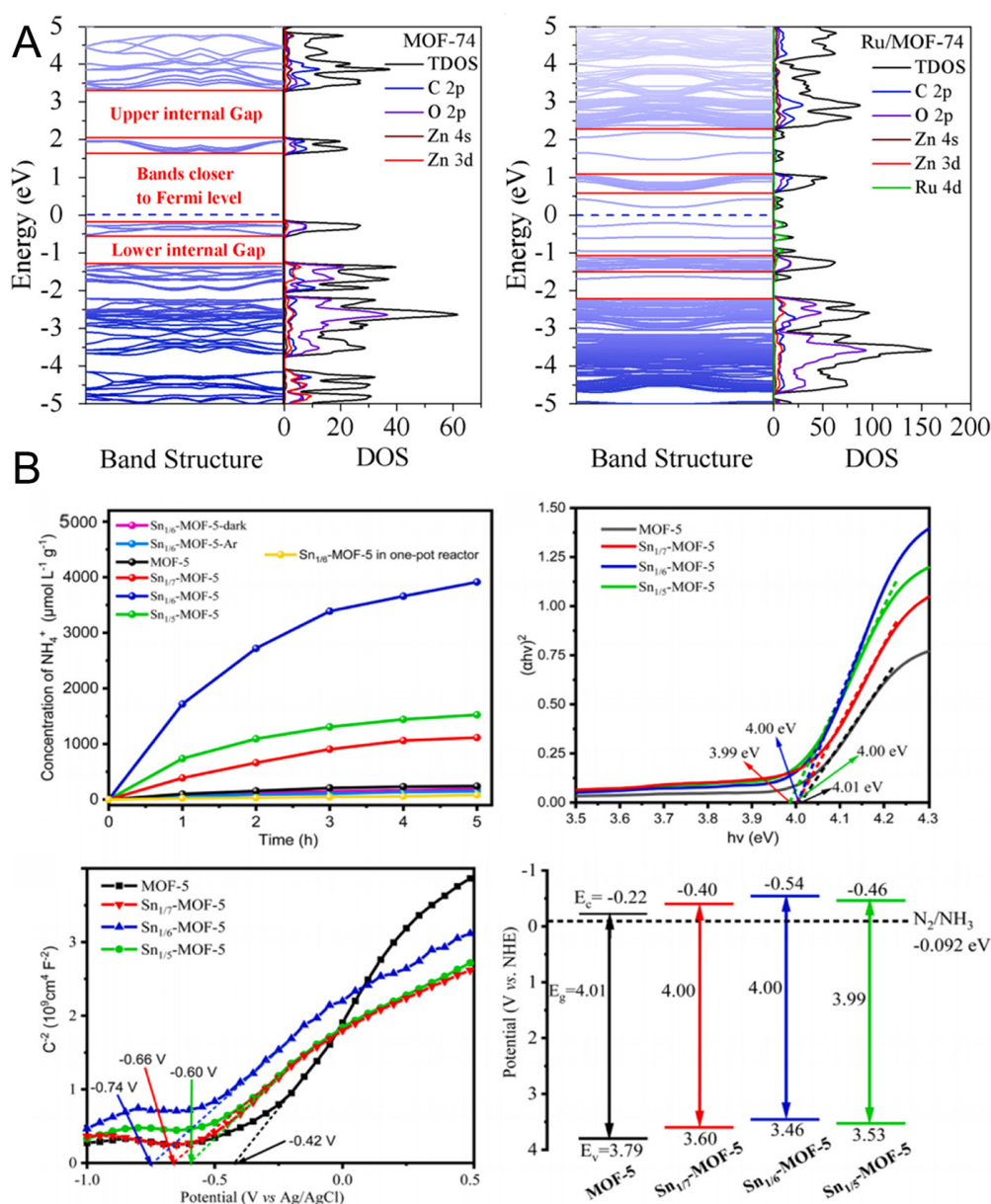


Figure 14. (A) Band structure (left) and DOS (right) of MOF-74 and Ru/MOF-74. Reproduced with permission Ref.^[143] Copyright 2023 Elsevier. (B) Photocatalytic activity of ammonia synthesis, corresponding spectra of $(\alpha h\nu)^2$ and $(h\nu)$, mott-Schottky plots and schematic diagram of the band gap of the materials. Reproduced with permission Ref.^[144] Copyright 2024 Elsevier.

distribution and energy levels of electron orbitals, researchers can improve light absorption, enhance charge carrier mobility, and optimize reactant activation, ultimately boosting photocatalytic efficiency.

Zhao *et al.* explored Cu doping to modulate the electronic structures of $\text{NH}_2\text{-MIL-125}$, improving its photocatalytic activity for nitrate reduction to ammonia^[147]. Cu^{2+} ions, introduced through an *in situ* solvothermal method, altered the band structure and increased electron density at Cu active sites, enhancing charge transfer and photocatalytic efficiency. As shown in Figure 16, density functional theory (DFT) calculations and *in situ* diffuse reflectance infrared Fourier transform (DRIFT) analysis revealed that Cu doping induced p-d hybridization between Cu 3d and NO_3^- O 2p orbitals, forming a stable bidentate

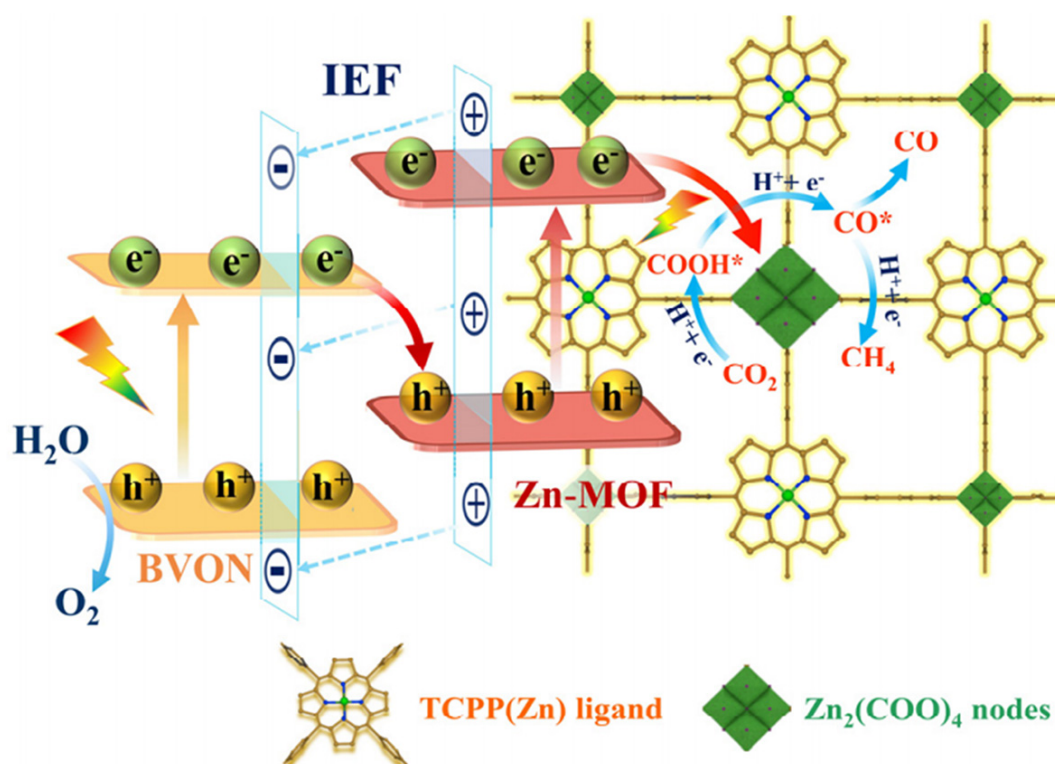


Figure 15. Schematic of photogenerated charges transfer in Zn-MOF/BVON heterojunctions during CO₂ photoreduction process. Reproduced with permission Ref.^[146] Copyright 2022 Elsevier.

adsorption structure for nitrates. This rehybridization lowered the activation energy barrier for nitrate reduction, achieving a high ammonia yield of 32.8 mg·g⁻¹·h⁻¹ and a selectivity of 94.8%.

Electron spin

Electron spin, a fundamental property of electrons, affects key aspects of photocatalytic performance in MOFs, including charge carrier generation, transfer, and recombination. In photocatalytic reactions, spin states influence reaction pathways and the stability of reactive intermediates, affecting overall efficiency. Electron spin also plays a role in radical-based reactions, where spin configuration determines reactivity and selectivity. By manipulating electron spin through strategies such as doping, functionalization, or structural design, researchers can significantly enhance MOF photocatalytic performance, making spin-engineering a valuable approach for advanced photocatalyst development.

Xu *et al.* synthesized defect-engineered titanium-based MOFs (MIL-125) to study the role of spin polarization in photocatalysis^[148]. The introduction of missing linkers and cluster defects created uneven charge distributions and increased the number of unpaired electrons, enhancing spin polarization around defect sites. Figure 17 illustrates the partial charge distributions, 3D spin polarization, and density of states, demonstrating that spin polarization elevated CB flexibility and increased free charge energy levels. These modifications facilitated efficient charge separation and surface reactions, enabling MIL-125-5% to achieve a hydrogen evolution rate of 16,507.27 μmol·g⁻¹·h⁻¹ and double the pollutant degradation efficiency of defect-free MIL-125. Shen *et al.* investigated MOFs with missing linker-cluster domain (MLCD) defects to evaluate their impact on the photocatalytic 2e⁻ oxygen reduction reaction (ORR) for hydrogen peroxide (H₂O₂) production^[149]. The introduction of MLCD defects induced spin polarization, which increased orbital-

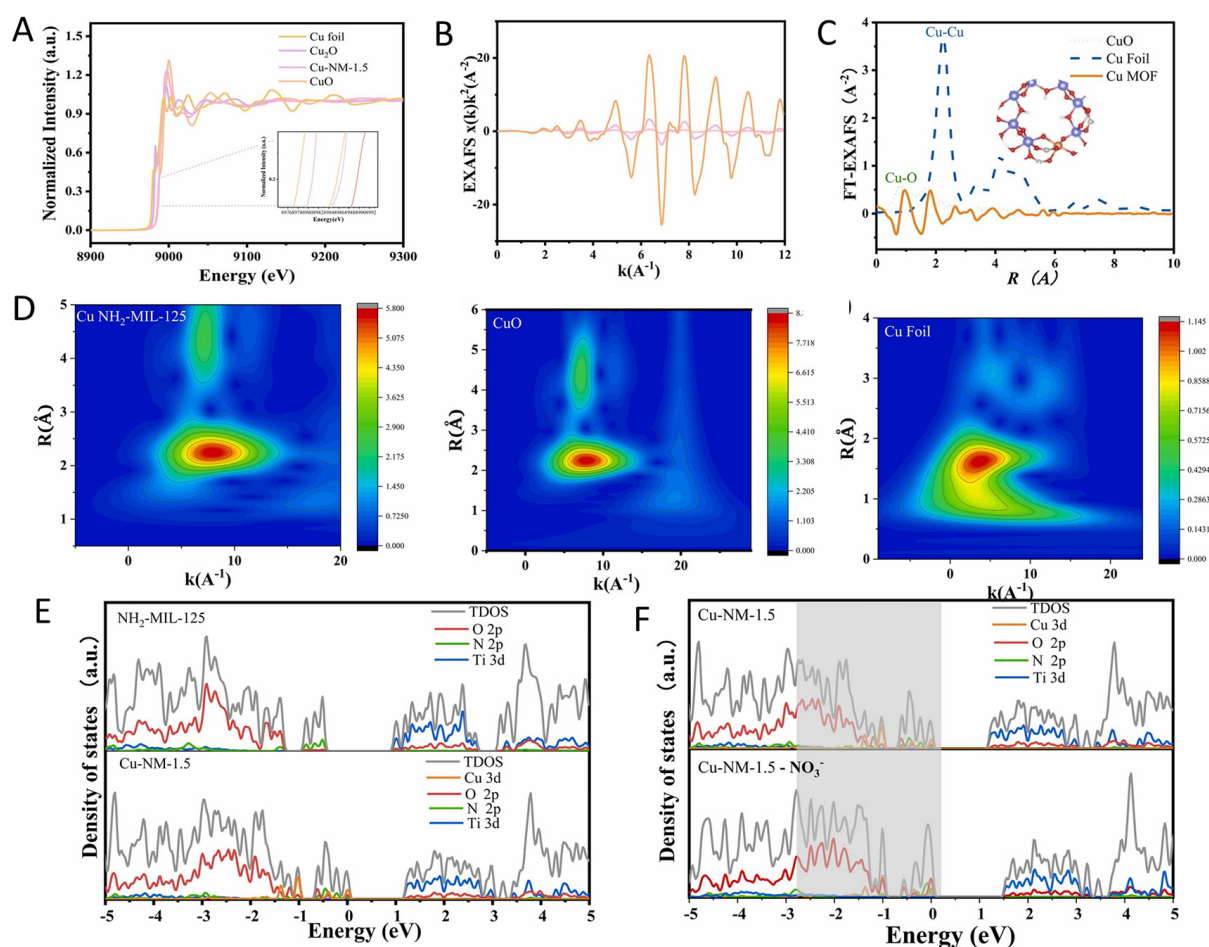


Figure 16. (A) XANES spectra at the Cu K-edge of Cu-NM-1.5 in the reference of Cu foil, Cu₂O, CuO; (B) EXAFS fitting results at R space; (C) Fourier transform of the Cu K-edge in the EXAFS of Cu-NM-1.5 (inset: Simulated coordination structure of the photocatalyst); (D) Wavelet transform analysis of Cu-NM-1.5 CuO and Cu foil; (E) DOS calculation results of Cu-NM-1.5 and NH₂-MIL-125; (F) DOS comparison before and after adsorption of nitrate ions over NH₂-MIL-125. Reproduced with permission Ref. [147] Copyright 2024 Elsevier.

limited resistance and disrupted interfacial charge transfer via the “Ti-O” bridge. These effects led to electron dissipation and reduced photocatalytic 2e⁻ ORR activity to 30% of its original performance.

SYNERGY OF MULTISCALE STRUCTURAL REGULATION

The photocatalytic performance of MOFs can be greatly enhanced by modulating their structures across different scales, from macro- and mesoscales to atomic and electronic levels. Each scale offers unique opportunities to optimize properties such as light absorption, charge transfer, active site accessibility, and stability. At macroscopic and mesoscopic scales, structural changes improve robustness, facilitate mass transport, and optimize interactions with reactants. At atomic and electronic levels, adjustments in metal ion coordination, ligand functionalization, and electronic structure enhance photocatalytic efficiency and charge carrier dynamics. The integration of these modifications across scales leads to synergistic effects, improving overall photocatalytic performance. This multiscale approach allows for the design of MOFs with tailored properties for energy conversion, environmental remediation, and sustainable chemical processes.

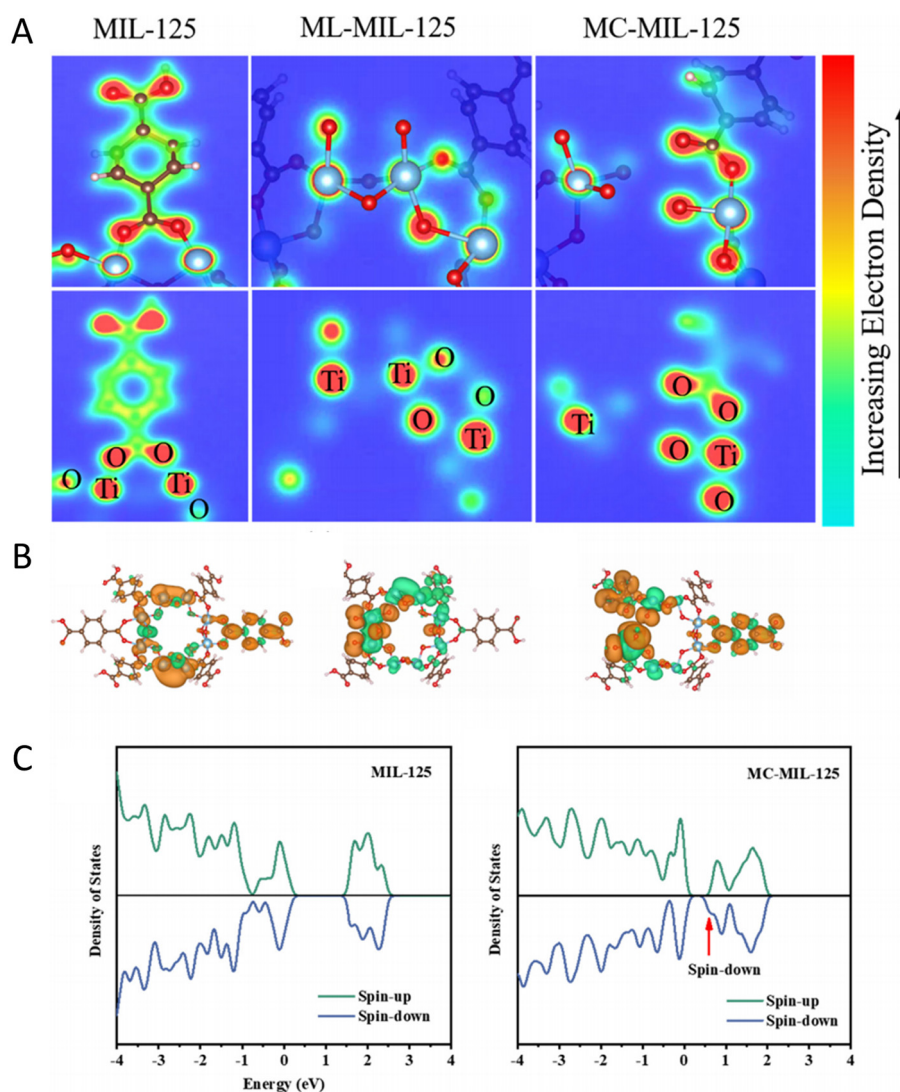


Figure 17. (A) The partial charge distributions of MIL-125, ML-MIL-125, and MC-MIL-125; (B) The 3D spatial spin polarizations of MIL-125, ML-MIL-125, and MC-MIL-125 (yellow and green represent spin-up and spin-down density, respectively); (C) Calculated total density of states (DOS) of MIL-125 and MC-MIL-125. Reproduced with permission Ref. [148] Copyright 2023 Elsevier.

Zhao *et al.* synthesized a 2D hierarchically porous (HP) MOF-Cu with a large lateral size using an amino-group-regulated hydrolysis strategy^[150]. The 3D MOF-Cu sheets were treated in ethanol/water at room temperature, leading to ligand replacement with -OH groups and the creation of defects, forming a 2D structure with enhanced photocatalytic activity. At the mesoscale, the 3D MOF-Cu was processed into a 2D structure, while at the atomic scale, defects induced structural changes in the ligands, and at the electronic scale, modifications in the band structure occurred [Figure 18]. The defective 2D HP MOF-Cu layer achieved a CO production rate 4.4 times higher than the original 3D MOF-Cu. This improvement was attributed to the synergy between atomic-scale defect creation and macroscopic morphology tuning, which narrowed the bandgap, broadened light absorption, and lowered the energy barrier for CO₂ reduction.

Li *et al.* developed a phosphorus-modified Ni-MOF-74/BiVO₄ S-scheme heterojunction for photocatalytic hydrogen evolution^[63]. The Ni-MOF-74 substrate, modified with Ni₂P nanoparticles, acted as an electron capture center, while the peanut-like BiVO₄ morphology facilitated efficient electron transfer. The

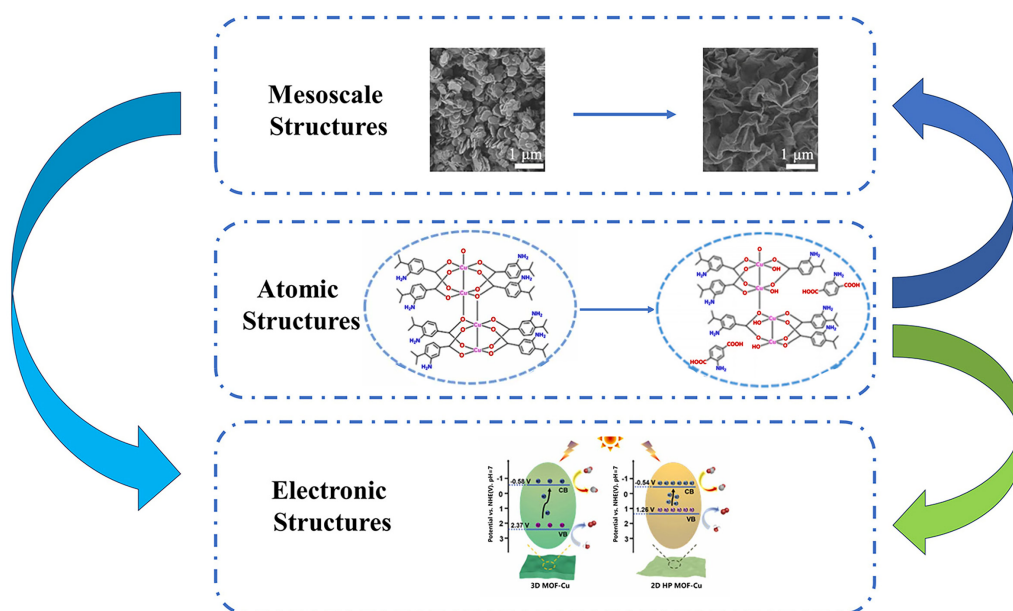


Figure 18. Synergy of Multiscale Regulation in MOF-Cu. Reproduced with permission Ref. [150] Copyright 2025 Elsevier.

integration of the 2D Ni-MOF-74 structure, Ni₂P's electron capture capability, and the S-scheme heterojunction enhanced directional carrier migration, resulting in a hydrogen production rate of 245.4 μmol in 5 h - 23 times higher than pure Ni-MOF-74. This work underscores the effectiveness of multiscale structural regulation in reducing charge recombination and improving carrier transfer.

PHOTOCATALYTIC APPLICATIONS OF TUNABLE STRUCTURES IN MOFS

Energy applications

MOFs have shown great potential in diverse energy-related photocatalytic applications. Through precise regulation of their structural and electronic properties, MOFs can efficiently utilize sunlight for clean energy production and energy storage. These capabilities make them attractive answers for addressing global energy challenges. As shown in Table 2, the following subsections explore key energy applications of MOFs in photocatalysis, highlighting their role in advancing sustainable energy solutions.

Photocatalytic hydrogen and oxygen evolution

Photocatalytic water splitting involves two key reactions: the HER and the oxygen evolution reaction (OER) [151]. In HER, photogenerated electrons reduce water to produce hydrogen gas, while in OER, photogenerated holes oxidize water to release oxygen. The efficiency of these reactions depends on the photocatalyst's ability to separate and transfer charges. OER is often the rate-limiting step due to its higher energy barrier. MOFs have gained attention as promising photocatalysts for water splitting due to their tunable metal sites, large surface area, and modifiable electronic properties, making them suitable for efficient hydrogen and oxygen evolution.

Hu *et al.* developed a highly efficient photocatalyst for hydrogen production by decorating CdS onto Zr-MOF using a pore functionalization strategy [Figure 19A] [134]. The mesoporous Zr-MOF was modified with thioglycolic acid, followed by S²⁻ anion exchange, allowing CdS to grow uniformly on the Zr-MOF surface, increasing active sites. This Zr-MOF-S@CdS composite achieved an impressive hydrogen evolution rate of 1,861.7 $\mu\text{mol}\cdot\text{g}^{-1}\cdot\text{h}^{-1}$, 4.5 times higher than pure CdS [Figure 19B]. Another study by Xu *et al.* used an *in situ* transformation strategy to convert Fe-based bimetallic MIL-88 MOFs into amorphous bimetallic

Table 2. Energy applications of MOF-based photocatalysts

Examples	MOFs-based photocatalysts	Impact of MOFs characteristics	Synthesis protocols	Ref.
Hydrogen evolution	Zr-MOF-S@CdS	High surface area and porous structure	Solvothermal at 120 °C for 48 h	[134]
Oxygen evolution	NiFe-OH-0.75	High surface area and porosity	Solvothermal at 120 °C for 5 h	[152]
CO ₂ reduction	ZIF-67-on-InOF-1	Hollow structure and heterogeneous interfaces	Solution precipitation Stirring at 70 °C for 20 min	[154]
	MOF-BiOBr/MCS	High specific surface area	Solvothermal at 180 °C for 6 h	[155]

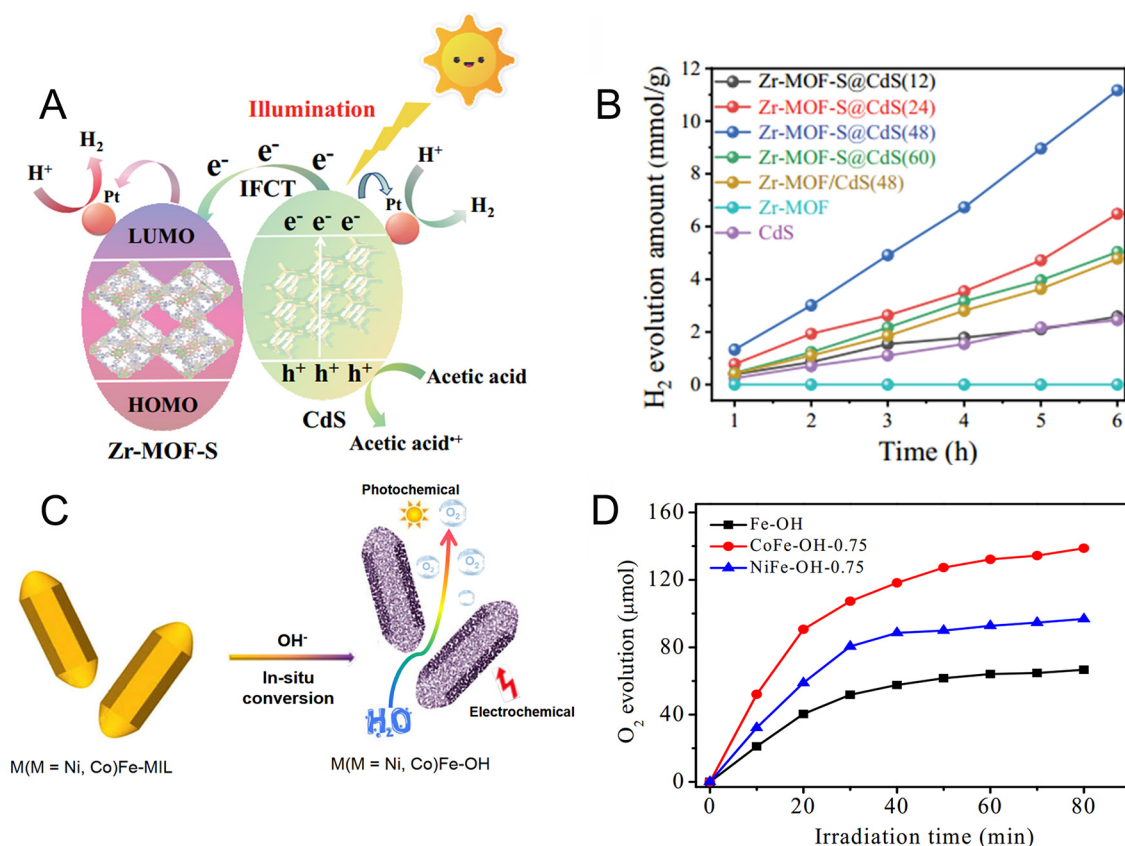


Figure 19. (A) Diagram of the photocatalytic mechanism of Zr-MOF-S@CdS; (B) Photocatalytic H₂ evolution amount. Reproduced with permission Ref. [134] Copyright 2022 Elsevier. (C) *In situ* formation of amorphous Fe-based bimetallic hydroxides from metal-organic frameworks as efficient oxygen evolution catalysts; (D) Time-dependent photocatalytic O₂ evolution over various cocatalysts by coupling with a [Ru(bpy)₃]Cl₂ photosensitizer. Reproduced with permission Ref. [152] Copyright 2021 Elsevier.

hydroxides, forming ultrasmall nanoparticles with abundant active sites^[152]. As shown in Figure 19C, the catalytic mechanism is driven by efficient OER, with active sites formed in the amorphous structure. The optimized NiFe-OH-0.75 catalyst achieved a current density of 10 mA cm⁻² with a small overpotential of 270 mV on glassy carbon electrodes, reduced to 235 mV on nickel foam substrates. Oxygen evolution efficiency comparison is shown in Figure 19D. These MOF-derived hydroxides also serve as effective cocatalysts for photocatalytic water oxidation when combined with appropriate photosensitizers.

Photocatalytic CO₂ reduction

Carbon dioxide reduction has always been a focal point in catalytic applications^[153]. Photocatalytic CO₂ reduction uses light energy to convert CO₂ into valuable chemicals such as carbon monoxide (CO) and hydrocarbons. The process generates electron-hole pairs when the photocatalyst absorbs light, with electrons reducing CO₂ at active sites and holes oxidizing water. As a sustainable method to reduce CO₂ emissions, this approach provides both environmental benefits and the production of renewable fuels, supporting the development of clean energy technologies.

Han *et al.* developed a MOF-derived hollow bimetallic oxide nanostructure, H-Co₃O₄/In₂O₃, for photocatalytic CO₂ reduction^[154]. The ZIF-67-on-InOF-1 heterostructure, created by growing Co-based ZIF-67 on InOF-1 nanorods, was treated with acid to form a hollow structure, increasing the surface area. This modification improved CO₂ adsorption and reaction efficiency [Figure 20]. The photocatalyst achieved a CO yield of $4,828 \pm 570 \mu\text{mol}\cdot\text{h}^{-1}\cdot\text{g}^{-1}$ and maintained stable performance over six consecutive runs. Hua *et al.* developed an S-scheme heterojunction photocatalyst, MOF-BiOBr/Mn_{0.2}Cd_{0.8}S (MOF-BiOBr/MCS), for visible-light-driven CO₂ reduction^[155]. The BiOBr nanosheets and Mn_{0.2}Cd_{0.8}S nanospheres were connected by an internal electric field, improving charge transfer and CO₂ adsorption. The optimized MOF-BiOBr/MCS composite achieved a CO evolution rate of $60.59 \mu\text{mol}\cdot\text{h}^{-1}\cdot\text{g}^{-1}$ under visible light.

Environmental applications

Beyond energy-related applications, MOFs have demonstrated significant potential in environmental photocatalysis. Their high surface area, tunable porosity, and capacity to generate reactive oxygen species (ROS) make them suitable for addressing critical environmental challenges^[156]. These include pollutant degradation, nitrogen fixation, and air quality improvement. As shown in Table 3, the following sections explore key environmental applications of MOFs in photocatalysis, highlighting their versatility and impact on sustainable environmental management.

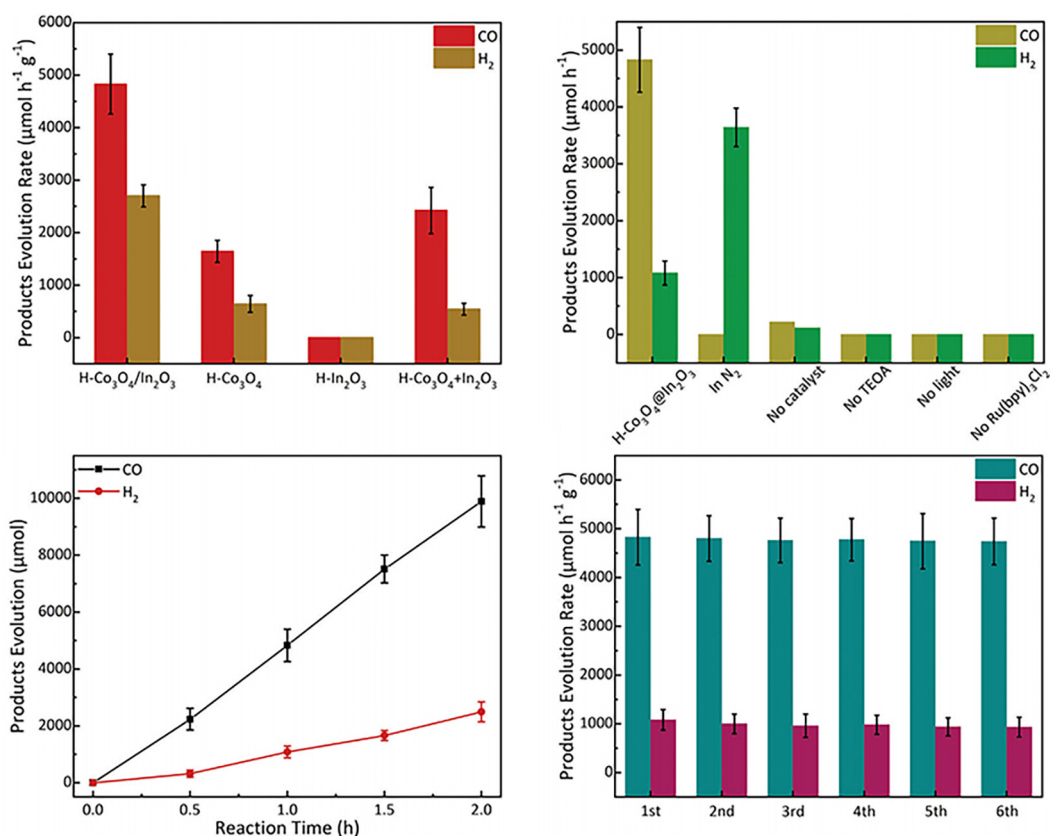
Photocatalytic hydrogen peroxide production

Photocatalytic H₂O₂ production involves reducing O₂ with photogenerated electrons to form O₂⁻ intermediates, which are protonated to yield H₂O₂. This light-driven process offers an energy-efficient and sustainable alternative to traditional industrial methods, which typically require high energy input and produce significant byproducts. By utilizing solar energy, photocatalytic H₂O₂ production supports renewable energy goals, producing a valuable chemical while reducing reliance on fossil fuels. Recent advancements in photocatalyst design have focused on improving efficiency, selectivity, and stability, making this process a promising route for sustainable energy conversion and chemical production.

As shown in Figure 21, Li *et al.* developed a hybrid photocatalyst combining polymeric carbon nitride (CN) with a 2D conductive Zn-containing MOF (Zn-MOF) for efficient H₂O₂ production^[157]. The photocatalytic activity of Zn-MOF was enhanced through annealing, which activated Zn sites and promoted the formation of key *OOH intermediates, crucial for the O₂ reduction process. The CN/Zn-MOF hybrid exhibited significantly improved H₂O₂ production under visible light irradiation, demonstrating its potential for sustainable chemical synthesis and energy applications by leveraging the synergistic properties of CN and Zn-MOF. Isaka *et al.* explored the photocatalytic production of H₂O₂ using MIL-125-NH₂ in a benzylalcohol/water two-phase system^[158]. The hydrophobization of MIL-125-NH₂ facilitated its separation from the aqueous phase, improving photocatalytic efficiency and enabling the simultaneous production of H₂O₂ and benzaldehyde. The system achieved spontaneous phase separation, allowing for high-concentration H₂O₂ production under visible light.

Table 3. Environmental applications of MOF-based photocatalysts

Examples	MOFs-based photocatalysts	Impact of MOF characteristics	Synthesis protocols	Ref.
Hydrogen peroxide production	Zn-MOF	2D morphology	Solution precipitation Stirring at 60 °C for 8 h	[157]
	MIL-125-NH ₂	Hydrophobization	Solvothermal at 150 °C for 16 h	[158]
Pollutant degradation	MOF@C@FeO	Nanopillared structure	Solvothermal at 160 °C for 12 h	[159]
	Bi/BiO _{2-x} -Bi ₂ O ₂ CO ₃ /BiOCl@Bi-MOF	High surface area and tunable structure	Solvothermal at 130 °C for 48 h	[160]
Nitrogen fixation	BMO/Bi-MOF	Large porosity	Solvothermal at 160 °C for 6 h	[161]
	Bi-MOF/g-C ₃ N ₄	High surface area and porous structure	Solvothermal at 120 °C for 20h	[162]
Nitrogen oxides reduction	rGO@ZnCo-ZIF	High surface area	Microwave at 140 °C for 30 min	[164]
	Yb-MOF/BiOBr	Large specific surface area and narrow band gap	Solution precipitation Stirring for 24 h	[165]

**Figure 20.** Photocatalytic CO₂ reduction of H-Co₃O₄/In₂O₃ and the control samples. Reproduced with permission Ref. [154] Copyright 2023 John Wiley and Sons.

Photocatalytic pollutant degradation

Pollutants in liquid and solid phases pose significant environmental challenges. Liquid-phase pollutants, such as organic dyes, pesticides, and heavy metals, are often resistant to traditional treatment methods and

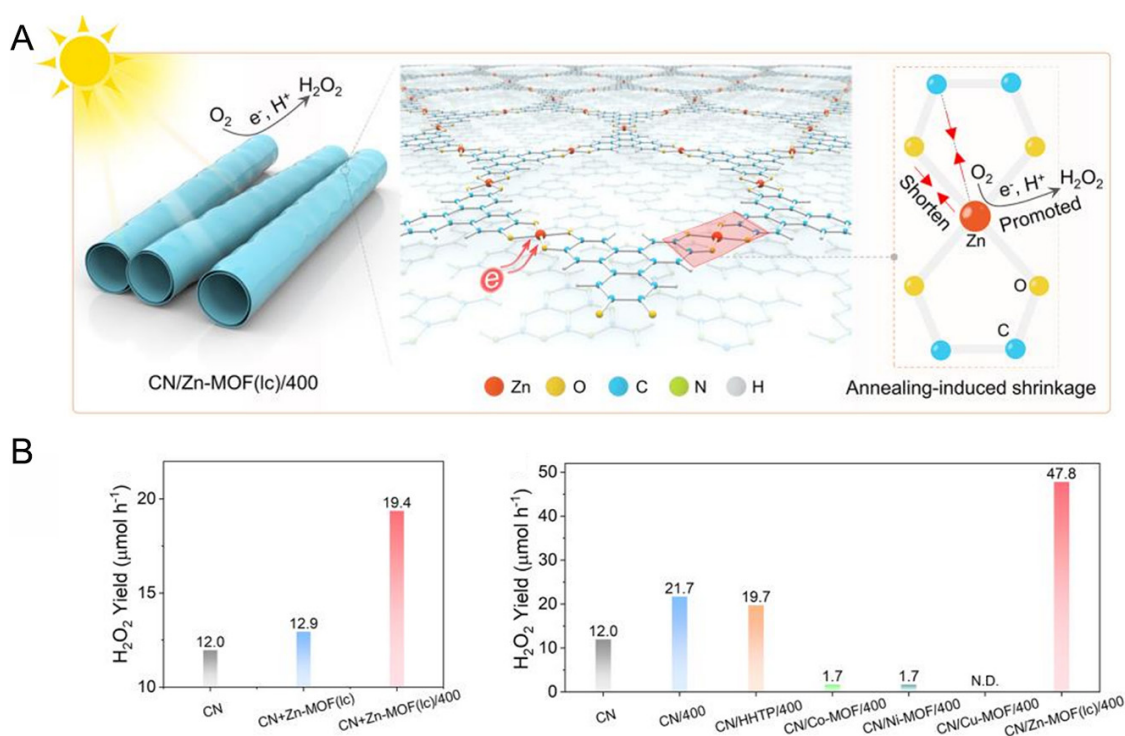


Figure 21. (A) An unlocked two-dimensional conductive Zn-MOF on polymeric carbon nitride for photocatalytic H_2O_2 production; (B) Activity comparison of a series of control samples. Reproduced with permission Ref. [157] Copyright 2023 John Wiley and Sons.

persist in wastewater. Solid-phase pollutants, including plastics and microplastics (MPs), contribute to soil and marine contamination. Photocatalysts generate ROS that break down pollutants into harmless byproducts, making this method ideal for environmental remediation. It uses renewable energy, operates under mild conditions, and avoids generating secondary waste, offering a green solution.

Haris *et al.* developed a nanopillared composite of 2D MOF and carbon-encapsulated iron oxide (C@FeO) for simultaneous removal of MPs and dissolved contaminants from water [159]. The 2D MOF@C@FeO composite featured a high surface area, abundant active sites, and magnetic properties, enabling the efficient removal of ~100% of MPs within 60 min and MB in a binary pollutant system. Additionally, the material exhibited excellent stability and reusability, retaining 90% of its removal capacity after six cycles. Zhang *et al.* constructed an indirect Z-type multicomponent heterojunction, $\text{Bi/BiO}_{2-x}\text{-Bi}_2\text{O}_2\text{CO}_3/\text{BiOCl@Bi-MOF}$, to enhance photocatalytic degradation of chlortetracycline (CTC), as shown in Figure 22 [160]. The composite, co-modified with plasma Bi and $\text{BiO}_{2-x}\text{-Bi}_2\text{O}_2\text{CO}_3$, achieved 94.6% degradation of CTC within 90 min under full-spectrum light. The enhanced performance was attributed to the synergistic interaction between the MOF structure and modified semiconductor components, which improved charge separation and photocatalytic efficiency.

Photocatalytic nitrogen fixation

Photocatalytic nitrogen fixation uses light energy to convert atmospheric N_2 into NH_3 , mimicking natural biological processes. Photogenerated electrons reduce N_2 at active sites on the photocatalyst, while holes oxidize water to produce protons that combine with nitrogen to form ammonia. Metal centers such as Fe, Mo, or Bi facilitate this process, offering a sustainable alternative to the energy-intensive Haber-Bosch method. This environmentally friendly approach reduces fossil fuel dependence, provides a greener route for ammonia production, and supports sustainable agriculture by lowering carbon emissions.

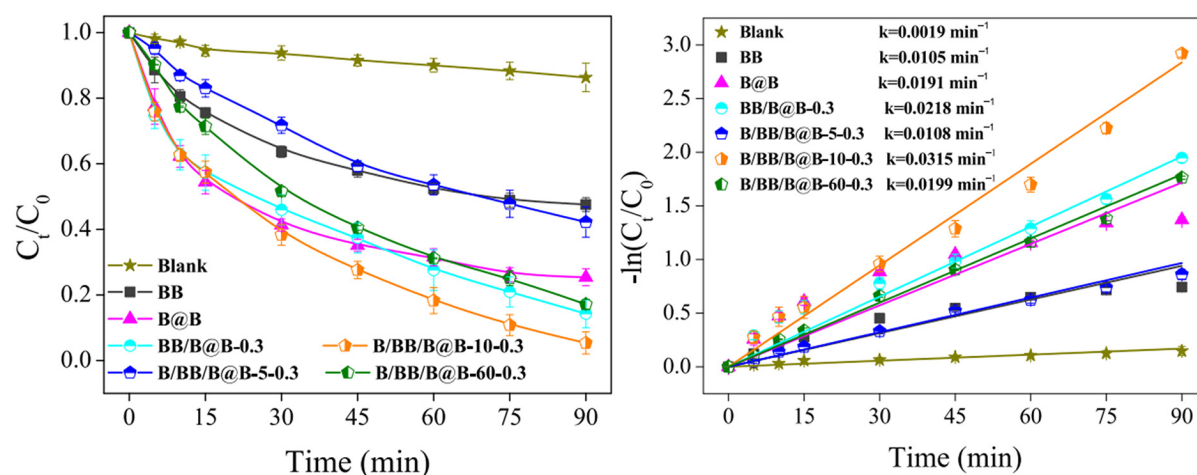


Figure 22. Photodegradation of CTC with B/BB/B@B-n-0.3 and its corresponding kinetic plots under full-spectrum light illumination. Reproduced with permission Ref. [160] Copyright 2023 Elsevier.

Dong *et al.* designed a Bi₂MoO₆/Bi-MOF composite photocatalyst with precisely regulated surface oxygen vacancies (OVs) in Bi-MOF to enhance ammonia synthesis^[161]. By reducing bismuth ions, the OV concentration was optimized, improving photoelectron transfer from Bi₂MoO₆ to Bi-MOF and facilitating N₂ activation at the Ovs [Figure 23]. The optimized photocatalyst achieved a remarkable ammonia yield of 125.78 μmol·h⁻¹·g⁻¹, 21.4 times higher than Bi₂MoO₆. Zhang *et al.* developed a Bi-MOF/g-C₃N₄ composite photocatalyst for simultaneous nitrogen fixation and pollutant degradation, aiming to convert wastewater into suitable irrigation water^[162]. The composite efficiently adsorbs nitrogen and organic pollutants, with g-C₃N₄ generating photocarriers under visible light. The hetero-interface between Bi-MOF and g-C₃N₄ facilitated efficient charge separation, enabling high ammonia yields and pollutant degradation rates.

Photocatalytic nitrogen oxide (NO_x) reduction

Photocatalytic nitrogen oxide (NO_x) reduction is an effective strategy to address air pollution caused by NO_x^[163], harmful pollutants from combustion, industrial activities, and vehicle emissions. In this process, light-induced electrons reduce NO_x species (such as NO and NO₂) to less harmful N₂ or other non-toxic products, while photogenerated holes oxidize water or organic compounds to enhance the reduction. Photocatalytic NO_x reduction provides a sustainable, energy-efficient solution to mitigate air pollution, improve urban air quality, and address environmental issues.

In one study, a mesocrystal ZnCo₂O₄ on reduced graphene oxide (rGO) composite photocatalyst for NO oxidation was developed^[164]. The rGO nanosheets improved the dispersity and conductivity of the composite, while mesoporous ZnCo₂O₄, optimized for visible-light absorption and an ideal Zn/Co ratio, served as the primary active site for NO oxidation. The composite demonstrated high photocatalytic activity, achieving 83.8% NO conversion under visible light and 92.6% under simulated solar light. Additionally, the material exhibited superior stability compared to N-doped TiO₂, highlighting its potential for long-term environmental remediation applications. Ai *et al.* developed an organic/inorganic Z-scheme heterojunction, Yb-MOF/BiOBr (Yb-MOF/BOB), to enhance photocatalytic NO removal under visible light [Figure 24]^[165]. The heterojunction combined the advantages of Yb-MOF and BiOBr, resulting in significantly improved photocatalytic performance. The Yb-MOF/BOB-20 composite achieved a NO

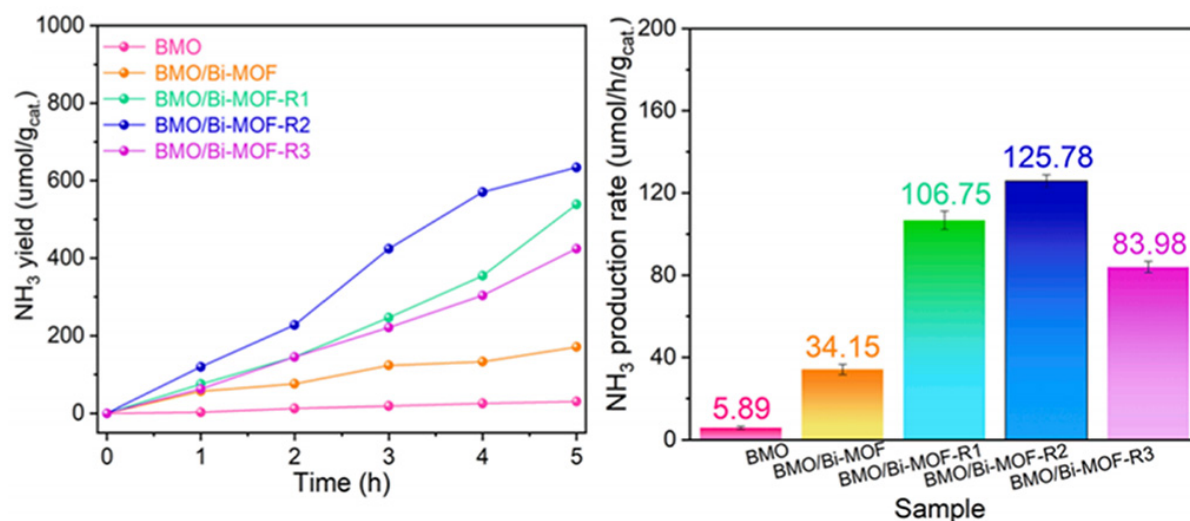


Figure 23. NH_3 yield and NH_3 production rate of BMO, BMO/Bi-MOF, BMO/Bi-MOF-R1, BMO/Bi-MOF-R2, and BMO/Bi-MOF-R3. Reproduced with permission Ref. [161] Copyright 2024 Elsevier.

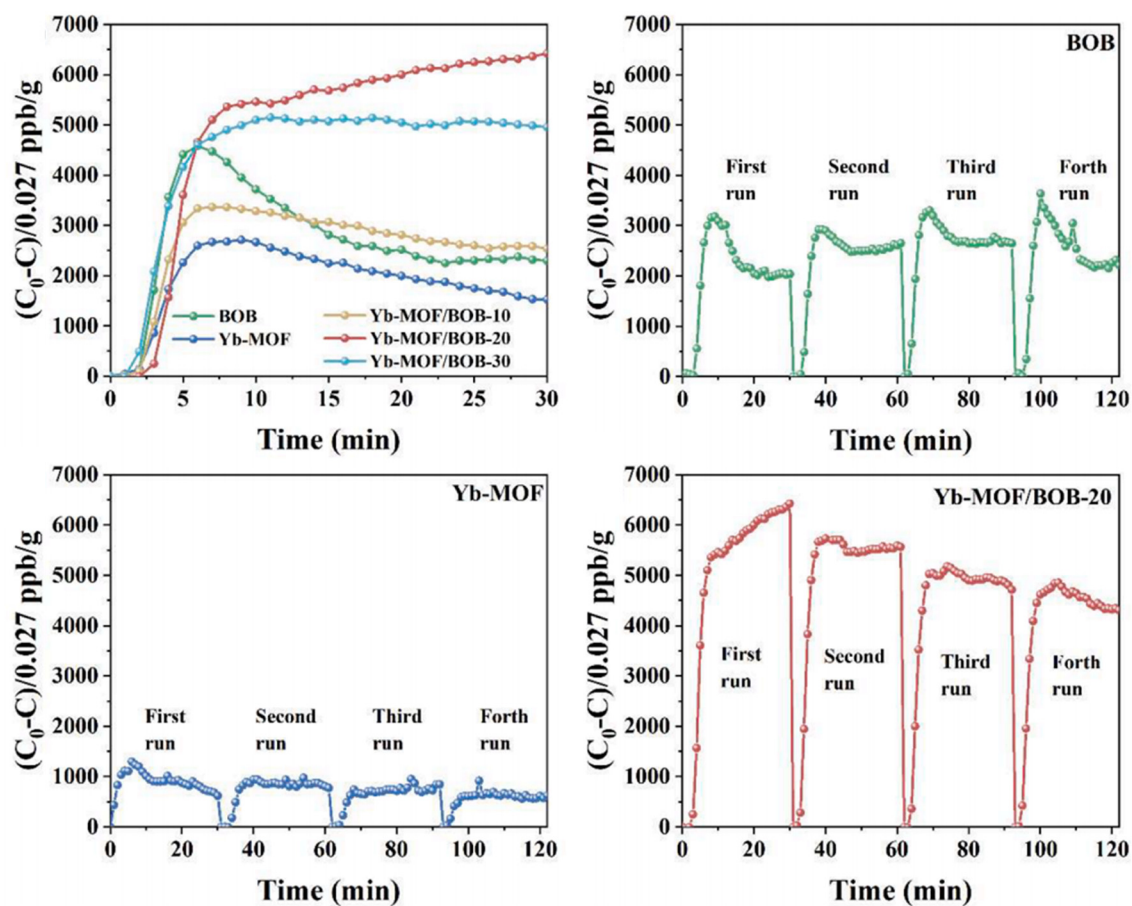


Figure 24. Visible light ($\lambda \geq 420$ nm) photocatalytic NO activity and cyclic photocatalytic performance of BOB, Yb-MOF and Yb-MOF/BOB-20. Reproduced with permission Ref. [165] Copyright 2024 Elsevier.

removal rate of 6,424 ppb/g, 2.8 times higher than pure BiOBr. This improvement was attributed to enhanced charge transfer and redox capacity facilitated by the Z-scheme structure.

CHALLENGES AND FUTURE PROSPECTS

As a highly tunable class of photocatalysts, MOFs present both significant opportunities and challenges for future development. Their unique structural versatility allows for precise control over photocatalytic properties, making them ideal for addressing global energy and environmental issues. The following are some challenges and future prospects.

Advanced electronic regulation

While electronic property regulation of MOFs is promising, maintaining the stability of these properties under real-world conditions, the complexity and cost of synthesis, limited reactivity under certain conditions, and the challenges of incorporating advanced features such as single-atom sites pose significant hurdles for their practical application. The inherent porosity and structural flexibility, while beneficial in some respects, may also lead to instability under operational conditions, limiting their long-term effectiveness in photocatalysis. The precise control of electronic properties remains crucial for enhancing photocatalytic performance, and future research could focus on developing MOFs that adapt their properties to external conditions, such as light intensity or reaction environments, and further optimize energy-level alignment and reaction specificity.

Multiscale simulation tools

Despite the potential of synergistic multiscale regulation, the inherent complexity of MOF structures and the unpredictable interactions between different structural scales often hinder the achievement of desired photocatalytic performance, complicating the design of efficient MOF-based systems. Future advancements could focus on developing multiscale simulation tools to better predict and optimize these interactions, while real-time monitoring using *in-situ* and operando techniques could help identify and address the complexities, ultimately facilitating the design of more efficient MOF-based photocatalytic systems.

Diversification of photocatalytic applications

The diversification of MOF applications in photocatalysis offers great potential, but challenges such as poor stability under harsh reaction conditions and high synthesis costs limit their widespread use. MOFs often degrade over time, losing active sites and reducing photocatalytic efficiency. Additionally, the complex and expensive synthesis processes hinder large-scale production. Future advancements could focus on enhancing the stability of MOFs through structural improvements and protective strategies, while reducing costs by optimizing synthesis methods and utilizing more abundant raw materials, enabling MOFs to be more effective and economically viable for various photocatalytic applications.

Integration with artificial intelligence

Integrating AI with MOF design offers significant promise for accelerating photocatalytic research, but challenges remain. Data availability and the need for high-quality MOF-specific datasets are key obstacles, as AI models require comprehensive and accurate data to make reliable predictions. Additionally, while AI can predict optimal structures, its effectiveness can be limited by the complexity of MOFs, which may not always align with AI's predictions in practical applications. Future research should focus on developing high-quality datasets and machine learning models tailored to photocatalysis, combining AI with advanced computational tools to optimize MOF design and overcome these challenges.

Collaborative advancements with emerging technologies

While integrating MOFs with emerging technologies such as photonic devices can enhance light absorption and charge transfer, the inherent complexity and compatibility issues of MOF structures pose significant challenges. Additionally, developing dynamic hybrid systems with MOFs can complicate system stability and performance. Overcoming these MOF-specific issues and achieving seamless integration at a large scale are crucial for unlocking their full potential in next-generation photocatalytic technologies.

Integration with hybrid-scale strategies

Currently, MOF research primarily focuses on single-scale strategies, with limited exploration of hybrid-scale approaches. The lack of attention to multiscale integration limits the full potential of MOFs. Integrating hybrid MOFs and exploring their properties are crucial for advancing the field. By bridging the gap between nano, micro, and macro scales, hybrid-scale strategies can significantly enhance photocatalytic efficiency by optimizing light absorption, charge carrier dynamics, and mass transport. Future research should prioritize the development of hybrid-scale strategies and focus on multiscale structural engineering to fully realize the potential of MOF-based photocatalysts.

CONCLUSION

In conclusion, photocatalysis has demonstrated transformative potential in sustainable energy conversion and environmental remediation, offering pathways for clean energy production and effective pollutant degradation. With their tunable structures and multifunctional properties, MOFs have emerged as a promising solution to overcome the limitations of conventional photocatalysts. Through systematic advancements in structural regulation across multiple scales - ranging from macro- and mesoscale architectures to atomic-scale coordination and electronic-scale properties - MOFs have achieved remarkable improvements in photocatalytic efficiency and adaptability. The synergistic effects of these multiscale regulations have expanded the applicability of MOFs in diverse fields, providing solutions for energy challenges and environmental issues. This comprehensive analysis underscores the critical role of MOFs in advancing photocatalyst design and highlights their potential as a cornerstone in the development of innovative and sustainable photocatalytic systems.

DECLARATIONS

Authors' contributions

Conceptualization, methodology, writing-original draft: Liu, J.; Gong, Z.

Software: Wu, D.; Liu, Y.

Writing-review & editing: Wang, J.; Zhang, Q.; Fu, C.

Supervision and funding acquisition: Fu, C.

Availability of data and materials

Not applicable.

Financial support and sponsorship

This work is supported by the Liaoning Applied Fundamental Research Project (Grant Nos. 2022JH2/101300158 and 2023JH2/101300014) and the Fundamental Research Funds for the Central Universities (Grant Nos. 3132024243 and 3132023506).

Conflicts of interest

All authors declared that there are no conflicts of interest.

Ethical approval and consent to participate

Not applicable.

Consent for publication

Not applicable.

Copyright

© The Author(s) 2025.

REFERENCES

1. Liu, T.; Wang, L.; Liu, X.; et al. Dynamic photocatalytic membrane coated with ZnIn_2S_4 for enhanced photocatalytic performance and antifouling property. *Chem. Eng. J.* **2020**, *379*, 122379. DOI
2. Li, R.; Heuer, J.; Kuckhoff, T.; Landfester, K.; Ferguson, C. T. J. pH-triggered recovery of organic polymer photocatalytic particles for the production of high value compounds and enhanced recyclability. *Angew. Chem. Int. Ed.* **2023**, *62*, e202217652. DOI PubMed
3. Shao, J.; Deng, K.; Chen, L.; et al. Aqueous synthesis of Nb-modified SnO_2 quantum dots for efficient photocatalytic degradation of polyethylene for *in situ* agricultural waste treatment. *Green. Process. Synth.* **2021**, *10*, 499-506. DOI
4. Liu, J.; Liang, L.; Su, B.; et al. Transformative strategies in photocatalyst design: merging computational methods and deep learning. *J. Mater. Inf.* **2024**, *4*, 33. DOI
5. Fei, H.; Wu, J.; Zhang, J.; et al. Photocatalytic performance and its internal relationship with hydration and carbonation of photocatalytic concrete: a review. *J. Build. Eng.* **2024**, *97*, 110782. DOI
6. Bui, V. K. H.; Nguyen, T. N.; Van Tran, V.; et al. Photocatalytic materials for indoor air purification systems: an updated mini-review. *Environ. Technol. Innov.* **2021**, *22*, 101471. DOI
7. Wang, Y.; Su, N.; Liu, J.; et al. Enhanced visible-light photocatalytic properties of SnO_2 quantum dots by niobium modification. *Results. Phys.* **2022**, *37*, 105515. DOI
8. Li, F.; Liu, G.; Liu, F.; Yang, S. A review of self-cleaning photocatalytic surface: effect of surface characteristics on photocatalytic activity for NO. *Environ. Pollut.* **2023**, *327*, 121580. DOI
9. Wu, T.; Yang, Y.; Zhao, Q.; et al. Photocatalytic membranes toward practical environmental remediation: fundamental, fabrication, and application. *Adv. Sustain. Syst.* **2024**, *8*, 2300374. DOI
10. Liu, J.; Zhang, Q.; Tian, X.; et al. Highly efficient photocatalytic degradation of oil pollutants by oxygen deficient SnO_2 quantum dots for water remediation. *Chem. Eng. J.* **2021**, *404*, 127146. DOI
11. Liu, Y.; Jiang, L.; Tian, Y.; et al. Covalent organic framework/ $\text{g-C}_3\text{N}_4$ van der Waals heterojunction toward H_2 production. *Inorg. Chem.* **2023**, *62*, 3271-7. DOI
12. Sun, H.; Shi, Y.; Shi, W.; Guo, F. High-crystalline/amorphous $\text{g-C}_3\text{N}_4$ S-scheme homojunction for boosted photocatalytic H_2 production in water/simulated seawater: interfacial charge transfer and mechanism insight. *Appl. Surf. Sci.* **2022**, *593*, 153281. DOI
13. Zhang, H.; Li, M. M. Crafting an active center with a local charge density gradient to facilitate photocatalytic ethylene production from CO_2 . *Curr. Opin. Green. Sustain. Chem.* **2022**, *36*, 100646. DOI
14. Wang, Q.; Wang, J.; Wang, J. C.; et al. Coupling CsPbBr_3 quantum dots with covalent triazine frameworks for visible-light-driven CO_2 reduction. *ChemSusChem* **2021**, *14*, 1131-9. DOI
15. Pei, W.; Zhang, W.; Yu, X.; et al. Computational design of spatially confined triatomic catalysts for nitrogen reduction reaction. *J. Mater. Inf.* **2023**, *3*, 26. DOI
16. Zhang, F.; Wang, X.; Liu, H.; et al. Recent advances and applications of semiconductor photocatalytic technology. *Appl. Sci.* **2019**, *9*, 2489. DOI
17. Ma, B.; Li, X.; Li, D.; Lin, K. A difunctional photocatalytic H_2 evolution composite co-catalyst tailored by integration with earth-abundant material and ultralow amount of noble metal. *Appl. Catal. B. Environ.* **2019**, *256*, 117865. DOI
18. Liu, J.; Qu, X.; Zhang, C.; et al. High-yield aqueous synthesis of partial-oxidized black phosphorus as layered nanodot photocatalysts for efficient visible-light driven degradation of emerging organic contaminants. *J. Clean. Prod.* **2022**, *377*, 134228. DOI
19. Wu, Y.; Zhong, L.; Yuan, J.; et al. Photocatalytic optical fibers for degradation of organic pollutants in wastewater: a review. *Environ. Chem. Lett.* **2021**, *19*, 1335-46. DOI
20. Bai, Y.; Hu, Z.; Jiang, J. X.; Huang, F. Hydrophilic conjugated materials for photocatalytic hydrogen evolution. *Chem. Asian. J.* **2020**, *15*, 1780-90. DOI PubMed
21. Wu, D.; Liu, X.; Liu, J.; Akhtar, A.; Fu, C. Hydrothermal synthesis of Z-scheme photocatalyst Zn_2SnO_4 - $\text{g-C}_3\text{N}_4$ for efficient tetracycline antibiotic removal. *Diam. Relat. Mater.* **2024**, *141*, 110572. DOI
22. Zhao, D.; Wu, X.; Gu, X.; Liu, J. Investigation into the degradation of air and runoff pollutants using nano $\text{g-C}_3\text{N}_4$ photocatalytic road surfaces. *Constr. Build. Mater.* **2024**, *411*, 134553. DOI
23. Yusuf, A. O.; Jitan, S. A.; Al Sakka, R.; et al. 3D printing to enable photocatalytic process engineering: a critical assessment and perspective. *Appl. Mater. Today.* **2023**, *35*, 101940. DOI

24. Lu, S.; Liu, H. Molecular doping on carbon nitride for efficient photocatalytic hydrogen production. *Langmuir* **2024**, *40*, 13331-8. DOI
25. Bui, V. K. H.; Tran, V. V.; Moon, J. Y.; Park, D.; Lee, Y. C. Titanium dioxide microscale and macroscale structures: a mini-review. *Nanomaterials* **2020**, *10*, 1190. DOI PubMed PMC
26. Wang, Y.; Wu, X.; Liu, J.; et al. Mo-modified band structure and enhanced photocatalytic properties of tin oxide quantum dots for visible-light driven degradation of antibiotic contaminants. *J. Environ. Chem. Eng.* **2022**, *10*, 107091. DOI
27. Luo, T.; Gilmanova, L.; Kaskel, S. Advances of MOFs and COFs for photocatalytic CO₂ reduction, H₂ evolution and organic redox transformations. *Coord. Chem. Rev.* **2023**, *490*, 215210. DOI
28. Younis, S. A.; Kwon, E. E.; Qasim, M.; et al. Metal-organic framework as a photocatalyst: progress in modulation strategies and environmental/energy applications. *Prog. Energy. Combust. Sci.* **2020**, *81*, 100870. DOI
29. Li, R.; Zhang, W.; Zhou, K. Metal-organic-framework-based catalysts for photoreduction of CO₂. *Adv. Mater.* **2018**, *30*, e1705512. DOI
30. Deng, Y.; Liu, J.; Zhou, Z.; et al. Recent advances in piezoelectric coupled with photocatalytic reaction system: synergistic mechanism, enhancement factors, and application. *ACS. Appl. Mater. Interfaces.* **2024**, *16*, 50071-95. DOI
31. Hamid, S. B. A.; Teh, S. J.; Lai, C. W. Photocatalytic water oxidation on ZnO: a review. *Catalysts* **2017**, *7*, 93. DOI
32. Tak, S.; Grewal, S.; Shreya; et al. Mechanistic insights and emerging trends in photocatalytic dye degradation for wastewater treatment. *Chem. Eng. Technol.* **2024**, *47*, e202400142. DOI
33. Gunawan, D.; Zhang, J.; Li, Q.; et al. Materials advances in photocatalytic solar hydrogen production: integrating systems and economics for a sustainable future. *Adv. Mater.* **2024**, *36*, e2404618. DOI
34. Liu, J.; Chen, L.; Cui, H.; Zhang, J.; Zhang, L.; Su, C. Y. Applications of metal-organic frameworks in heterogeneous supramolecular catalysis. *Chem. Soc. Rev.* **2014**, *43*, 6011-61. DOI
35. Zhang, T.; Jin, Y.; Shi, Y.; Li, M.; Li, J.; Duan, C. Modulating photoelectronic performance of metal-organic frameworks for premium photocatalysis. *Coord. Chem. Rev.* **2019**, *380*, 201-29. DOI
36. Shen, Y.; Pan, T.; Wang, L.; Ren, Z.; Zhang, W.; Huo, F. Programmable logic in metal-organic frameworks for catalysis. *Adv. Mater.* **2021**, *33*, e2007442. DOI
37. Gao, Z.; Iqbal, A.; Hassan, T.; Zhang, L.; Wu, H.; Koo, C. M. Texture regulation of metal-organic frameworks, microwave absorption mechanism-oriented structural optimization and design perspectives. *Adv. Sci.* **2022**, *9*, e2204151. DOI PubMed PMC
38. Liu, Y.; Huang, D.; Cheng, M.; et al. Metal sulfide/MOF-based composites as visible-light-driven photocatalysts for enhanced hydrogen production from water splitting. *Coord. Chem. Rev.* **2020**, *409*, 213220. DOI
39. Saboor F, Shahsavari S, Zandjou M, Asgari M. From structure to catalysis: advances in metal-organic frameworks-based shape-selective reactions. *ChemNanoMat* **2024**, *10*, e202400049. DOI
40. Cui, Y.; Zhao, Y.; Wu, J.; Hou, H. Recent discussions on homogeneous host-guest metal-organic framework composites in synthesis and catalysis. *Nano. Today.* **2023**, *52*, 101972. DOI
41. Zhan, W.; Sun, L.; Han, X. Recent progress on engineering highly efficient porous semiconductor photocatalysts derived from metal-organic frameworks. *Nanomicro. Lett.* **2019**, *11*, 1. DOI PubMed PMC
42. Tasleem, S.; Tahir, M.; Khalifa, W. A. Current trends in structural development and modification strategies for metal-organic frameworks (MOFs) towards photocatalytic H₂ production: a review. *Int. J. Hydrogen. Energy.* **2021**, *46*, 14148-89. DOI
43. Dhakshinamoorthy, A.; Li, Z.; Garcia, H. Catalysis and photocatalysis by metal organic frameworks. *Chem. Soc. Rev.* **2018**, *47*, 8134-72. DOI PubMed
44. Zhang, M. Y.; Li, J. K.; Wang, R.; Zhao, S. N.; Zang, S. Q.; Mak, T. C. W. Construction of core-shell MOF@COF hybrids with controllable morphology adjustment of COF shell as a novel platform for photocatalytic cascade reactions. *Adv. Sci.* **2021**, *8*, e2101884. DOI PubMed PMC
45. Qin, J.; Dou, Y.; Zhou, J.; et al. Encapsulation of carbon-nanodots into metal-organic frameworks for boosting photocatalytic upcycling of polyvinyl chloride plastic. *Appl. Catal. B. Environ.* **2024**, *341*, 123355. DOI
46. Shi, Y.; Zou, Y.; Khan, M. S.; et al. Metal-organic framework-derived photoelectrochemical sensors: structural design and biosensing technology. *J. Mater. Chem. C.* **2023**, *11*, 3692-709. DOI
47. Jiang, S.; Li, X. L.; Fang, D.; et al. Metal-organic-framework-derived 3D hierarchical matrixes for high-performance flexible Li-S batteries. *ACS. Appl. Mater. Interfaces.* **2023**, *15*, 20064-74. DOI
48. Han, B.; Li, F. Regulating the electrocatalytic performance for nitrogen reduction reaction by tuning the N contents in Fe₃@N_xC_{20-x} (x = 0~4): a DFT exploration. *J. Mater. Inf.* **2023**, *3*, 24. DOI
49. Khan, M. S.; Li, Y.; Li, D. S.; Qiu, J.; Xu, X.; Yang, H. Y. A review of metal-organic framework (MOF) materials as an effective photocatalyst for degradation of organic pollutants. *Nanoscale. Adv.* **2023**, *5*, 6318-48. DOI PubMed PMC
50. Khan, M. S.; Zhu, S.; Chen, S. B. Metal-organic frameworks (MOFs) for oxo-anion removal in wastewater treatment: advancements and applications. *Chem. Eng. J.* **2024**, *500*, 157396. DOI
51. Li, X.; He, Y.; Chen, J.; Li, Q.; Liu, P.; Li, J. Recent advances in rational design, synthesis and application of metal-organic frameworks as visible-light-driven photocatalysts. *Inorg. Chem. Front.* **2024**, *11*, 6794-852. DOI
52. Doustkhah, E.; Esmat, M.; Fukata, N.; Ide, Y.; Hanaor, D. A. H.; Assadi, M. H. N. MOF-derived nanocrystalline ZnO with controlled orientation and photocatalytic activity. *Chemosphere* **2022**, *303*, 134932. DOI PubMed
53. Chen, Y.; Zhai, B.; Liang, Y.; Li, Y.; Li, J. Preparation of CdS/g-C₃N₄/MOF composite with enhanced visible-light photocatalytic

- activity for dye degradation. *J. Solid. State. Chem.* **2019**, *274*, 32-9. DOI
54. Dong, W.; Jia, J.; Wang, Y.; et al. Visible-light-driven solvent-free photocatalytic CO₂ reduction to CO by Co-MOF/Cu₂O heterojunction with superior selectivity. *Chem. Eng. J.* **2022**, *438*, 135622. DOI
55. Alvaro, M.; Carbonell, E.; Ferrer, B.; Llabrés, X. F. X.; Garcia, H. Semiconductor behavior of a metal-organic framework (MOF). *Chemistry* **2007**, *13*, 5106-12. DOI PubMed
56. Zhu, C.; Hou, J.; Wang, X.; et al. Optimizing ligand-to-metal charge transfer in metal-organic frameworks to enhance photocatalytic performance. *Chem. Eng. J.* **2024**, *499*, 156527. DOI
57. Bhattacharyya, A.; Gutiérrez, M.; Cohen, B.; Valverde-González, A.; Iglesias, M.; Douhal, A. How does the metal doping in mixed metal MOFs influence their photodynamics? A direct evidence for improved photocatalysts. *Mater. Today. Energy.* **2022**, *29*, 101125. DOI
58. Mao, S.; Shi, J.; Sun, G.; et al. Au nanodots@thiol-UiO66@ZnIn₂S₄ nanosheets with significantly enhanced visible-light photocatalytic H₂ evolution: the effect of different Au positions on the transfer of electron-hole pairs. *Appl. Catal. B. Environ.* **2021**, *282*, 119550. DOI
59. Mao, S.; Zou, Y.; Sun, G.; et al. Thio linkage between CdS quantum dots and UiO-66-type MOFs as an effective transfer bridge of charge carriers boosting visible-light-driven photocatalytic hydrogen production. *J. Colloid. Interface. Sci.* **2021**, *581*, 1-10. DOI
60. Wang, C.; Wang, X.; Liu, W. The synthesis strategies and photocatalytic performances of TiO₂/MOFs composites: a state-of-the-art review. *Chem. Eng. J.* **2020**, *391*, 123601. DOI
61. Chen, Z.; Cao, L.; Liu, A.; et al. Modulating the band gap of a pyrazinoquinoxaline-based metal-organic framework through orbital hybridization for enhanced visible light-driven C=N bond construction. *J. Mater. Chem. A.* **2024**, *12*, 30582-90. DOI
62. Wang, C.; Yi, X.; Wang, P. Powerful combination of MOFs and C₃N₄ for enhanced photocatalytic performance. *Appl. Catal. B. Environ.* **2019**, *247*, 24-48. DOI
63. Li, H.; Gong, H.; Jin, Z. Phosphorus modified Ni-MOF-74/BiVO₄ S-scheme heterojunction for enhanced photocatalytic hydrogen evolution. *Appl. Catal. B. Environ.* **2022**, *307*, 121166. DOI
64. Gorle, D. B.; Ponnada, S.; Kiai, M. S.; et al. Review on recent progress in metal-organic framework-based materials for fabricating electrochemical glucose sensors. *J. Mater. Chem. B.* **2021**, *9*, 7927-54. DOI
65. Wen, C.; Li, R.; Chang, X.; Li, N. Metal-organic frameworks-based optical nanosensors for analytical and bioanalytical applications. *Biosensors* **2023**, *13*, 128. DOI PubMed PMC
66. Du, J.; Shi, F.; Wang, K.; et al. Metal-organic framework-based biosensing platforms for diagnosis of bacteria-induced infectious diseases. *TrAC-Trend. Anal. Chem.* **2024**, *175*, 117707. DOI
67. Cai, C.; Fan, G.; Du, B.; et al. Metal-organic-framework-based photocatalysts for microorganism inactivation: a review. *Catal. Sci. Technol.* **2022**, *12*, 3767-77. DOI
68. Pan, Y.; Abazari, R.; Yao, J.; Gao, J. Recent progress in 2D metal-organic framework photocatalysts: synthesis, photocatalytic mechanism and applications. *J. Phys. Energy.* **2021**, *3*, 032010. DOI
69. Xiao, J. D.; Li, R.; Jiang, H. L. Metal-organic framework-based photocatalysis for solar fuel production. *Small. Methods.* **2023**, *7*, e2201258. DOI
70. Liu, Y.; Zhao, M.; Ren, Y.; et al. Linker-exchanged zeolitic imidazolate framework membranes for efficient CO₂ separation. *J. Membr. Sci.* **2024**, *697*, 122568. DOI
71. Zahir, I. M.; Waqas, K. M.; Shaheen, M.; et al. 1,2,4,5-benzene-tetra-carboxylic acid and 2-methylimidazole bi-linker intercalated redox active copper organic framework for advanced battery-supercapacitor hybrids. *J. Electroanal. Chem.* **2023**, *941*, 117505. DOI
72. Kamal, S.; Khalid, M.; Khan, M. S.; Shahid, M. Metal organic frameworks and their composites as effective tools for sensing environmental hazards: an up to date tale of mechanism, current trends and future prospects. *Coord. Chem. Rev.* **2023**, *474*, 214859. DOI
73. Tranchemontagne, D. J.; Mendoza-Cortés, J. L.; O'Keeffe, M.; Yaghi, O. M. Secondary building units, nets and bonding in the chemistry of metal-organic frameworks. *Chem. Soc. Rev.* **2009**, *38*, 1257-83. DOI PubMed
74. Mandal, S.; Yoosefi, S.; Mengele, A. K.; Rau, S.; Pannwitz, A. Active molecular units in metal organic frameworks for artificial photosynthesis. *Inorg. Chem. Front.* **2024**, *11*, 7682-755. DOI
75. Kalmutzki, M. J.; Hanikel, N.; Yaghi, O. M. Secondary building units as the turning point in the development of the reticular chemistry of MOFs. *Sci. Adv.* **2018**, *4*, eaat9180. DOI PubMed PMC
76. Li, N.; Zhang, W.; Wang, D.; Li, G.; Zhao, Y. Synthesis and applications of TiO₂-based nanostructures as photocatalytic materials. *Chem. Asian. J.* **2022**, *17*, e202200822. DOI
77. Wu, X.; Xie, S.; Zhang, H.; Zhang, Q.; Sels, B. F.; Wang, Y. Metal sulfide photocatalysts for lignocellulose valorization. *Adv. Mater.* **2021**, *33*, e2007129. DOI
78. Ma, J.; Liu, K.; Yang, X.; et al. Recent advances and challenges in photoreforming of biomass-derived feedstocks into hydrogen, biofuels, or chemicals by using functional carbon nitride photocatalysts. *ChemSusChem* **2021**, *14*, 4903-22. DOI PubMed
79. Zulfa, L. L.; Ediaty, R.; Hidayat, A. R. P.; et al. Synergistic effect of modified pore and heterojunction of MOF-derived α -Fe₂O₃/ZnO for superior photocatalytic degradation of methylene blue. *RSC. Adv.* **2023**, *13*, 3818-34. DOI PubMed PMC
80. Gu, Z. G.; Li, D. J.; Zheng, C.; Kang, Y.; Wöll, C.; Zhang, J. MOF-templated synthesis of ultrasmall photoluminescent carbon-nanodot arrays for optical applications. *Angew. Chem. Int. Ed.* **2017**, *56*, 6853-8. DOI PubMed
81. Ma, X.; Liu, H.; Yang, W.; Mao, G.; Zheng, L.; Jiang, H. L. Modulating coordination environment of single-atom catalysts and their

- proximity to photosensitive units for boosting MOF photocatalysis. *J. Am. Chem. Soc.* **2021**, *143*, 12220-9. DOI
82. Zhuang, X.; Zhang, S.; Tang, Y.; Yu, F.; Li, Z.; Pang, H. Recent progress of MOF/MXene-based composites: synthesis, functionality and application. *Coord. Chem. Rev.* **2023**, *490*, 215208. DOI
83. Liu, C.; Wang, J.; Wan, J.; Yu, C. MOF-on-MOF hybrids: synthesis and applications. *Coord. Chem. Rev.* **2021**, *432*, 213743. DOI
84. Guo, J.; Liang, Y.; Liu, L.; et al. Noble-metal-free CdS/Ni-MOF composites with highly efficient charge separation for photocatalytic H₂ evolution. *Appl. Surf. Sci.* **2020**, *522*, 146356. DOI
85. Ma, Y.; Fang, H.; Chen, R.; et al. 2D-MOF/2D-MOF heterojunctions with strong hetero-interface interaction for enhanced photocatalytic hydrogen evolution. *Rare. Met.* **2023**, *42*, 3993-4004. DOI
86. Kang, D. Y.; Lee, J. S. Challenges in developing MOF-based membranes for gas separation. *Langmuir* **2023**, *39*, 2871-80. DOI PubMed
87. Roohollahi, H.; Zeinalzadeh, H.; Kazemian, H. Recent advances in adsorption and separation of methane and carbon dioxide greenhouse gases using metal-organic framework-based composites. *Ind. Eng. Chem. Res.* **2022**, *61*, 10555-86. DOI
88. Ali, M.; Pervaiz, E.; Noor, T.; Rabi, O.; Zahra, R.; Yang, M. Recent advancements in MOF-based catalysts for applications in electrochemical and photoelectrochemical water splitting: a review. *Int. J. Energy. Res.* **2021**, *45*, 1190-226. DOI
89. Li, D.; Kassymova, M.; Cai, X.; Zang, S.; Jiang, H. Photocatalytic CO₂ reduction over metal-organic framework-based materials. *Coord. Chem. Rev.* **2020**, *412*, 213262. DOI
90. Yue, C.; Chen, L.; Zhang, H.; et al. Metal-organic framework-based materials: emerging high-efficiency catalysts for the heterogeneous photocatalytic degradation of pollutants in water. *Environ. Sci. Water. Res. Technol.* **2023**, *9*, 669-95. DOI
91. Yang, S. J.; Im, J. H.; Kim, T.; Lee, K.; Park, C. R. MOF-derived ZnO and ZnO@C composites with high photocatalytic activity and adsorption capacity. *J. Hazard. Mater.* **2011**, *186*, 376-82. DOI
92. Zhang, C. F.; Qiu, L. G.; Ke, F.; et al. A novel magnetic recyclable photocatalyst based on a core-shell metal-organic framework Fe₃O₄@MIL-100(Fe) for the decolorization of methylene blue dye. *J. Mater. Chem. A* **2013**, *1*, 14329-34. DOI
93. Li, Z.; Zhang, M.; Liu, B.; Guo, C.; Zhou, M. Rapid fabrication of metal-organic framework thin films using in situ microwave irradiation and its photocatalytic property. *Inorg. Chem. Commun.* **2013**, *36*, 241-4. DOI
94. Saha, S.; Das, G.; Thote, J.; Banerjee, R. Photocatalytic metal-organic framework from CdS quantum dot incubated luminescent metallohydrogel. *J. Am. Chem. Soc.* **2014**, *136*, 14845-51. DOI PubMed
95. Fu, Y.; Sun, D.; Chen, Y.; et al. An amine-functionalized titanium metal-organic framework photocatalyst with visible-light-induced activity for CO₂ reduction. *Angew. Chem. Int. Ed.* **2012**, *51*, 3364-7. DOI
96. Fang, X.; Shang, Q.; Wang, Y.; et al. Single Pt atoms confined into a metal-organic framework for efficient photocatalysis. *Adv. Mater.* **2018**, *30*, 1705112. DOI
97. Nasalevich, M. A.; Hendon, C. H.; Santaclara, J. G.; et al. Electronic origins of photocatalytic activity in d⁰ metal organic frameworks. *Sci. Rep.* **2016**, *6*, 23676. DOI PubMed PMC
98. Yang, W.; Wang, H. J.; Liu, R. R.; et al. Tailoring crystal facets of metal-organic layers to enhance photocatalytic activity for CO₂ reduction. *Angew. Chem. Int. Ed.* **2021**, *60*, 409-14. DOI
99. Shen, L.; Liang, S.; Wu, W.; Liang, R.; Wu, L. CdS-decorated UiO-66(NH₂) nanocomposites fabricated by a facile photodeposition process: an efficient and stable visible-light-driven photocatalyst for selective oxidation of alcohols. *J. Mater. Chem. A* **2013**, *1*, 11473-82. DOI
100. Zhang, C.; Xie, C.; Gao, Y.; et al. Charge separation by creating band bending in metal-organic frameworks for improved photocatalytic hydrogen evolution. *Angew. Chem. Int. Ed.* **2022**, *61*, e202204108. DOI
101. Wang, W.; Zhang, L.; Wang, W.; Huang, J.; Wu, Q.; Wu, J. J. Photocatalytic degradation of 1,4-dioxane by heterostructured Bi₂O₃/Cu-MOF composites. *Catalysts* **2023**, *13*, 1211. DOI
102. Deng, X.; Yang, L.; Huang, H.; et al. Shape-defined hollow structural Co-MOF-74 and Metal nanoparticles@Co-MOF-74 composite through a transformation strategy for enhanced photocatalysis performance. *Small* **2019**, *15*, e1902287. DOI
103. Meng, R.; Lu, Y.; Zou, L.; et al. Growth of TiO₂/Ti-MOF nanorod array with enhanced photoabsorption and photocatalytic properties on carbon cloth for efficient auto-cleaning solar desalination. *Desalination* **2024**, *578*, 117455. DOI
104. Wang, Z.; He, M.; Jiang, H.; He, H.; Qi, J.; Ma, J. Photocatalytic MOF membranes with two-dimensional heterostructure for the enhanced removal of agricultural pollutants in water. *Chem. Eng. J.* **2022**, *435*, 133870. DOI
105. Gao, Y.; Yi, X.; Wang, C.; Wang, F.; Wang, P. Effective Cr(VI) reduction over high throughput Bi-BDC MOF photocatalyst. *Mater. Res. Bull.* **2023**, *158*, 112072. DOI
106. Liang, J.; Yu, H.; Shi, J.; Li, B.; Wu, L.; Wang, M. Dislocated bilayer MOF Enables high-selectivity photocatalytic reduction of CO₂ to CO. *Adv. Mater.* **2023**, *35*, e2209814. DOI
107. Song, M.; Song, X.; Liu, X.; Zhou, W.; Huo, P. Enhancing photocatalytic CO₂ reduction activity of ZnIn₂S₄/MOF-808 microsphere with S-scheme heterojunction by in situ synthesis method. *Chin. J. Catal.* **2023**, *51*, 180-92. DOI
108. Chen, L.; Wang, X.; Rao, Z.; et al. One-pot Synthesis of the MIL-100 (Fe) MOF/MOX homojunctions with tunable hierarchical pores for the photocatalytic removal of BTXS. *Appl. Catal. B. Environ.* **2022**, *303*, 120885. DOI
109. Yuan, L.; Zhang, C.; Zou, Y.; et al. A S-scheme MOF-on-MOF heterostructure. *Adv. Funct. Mater.* **2023**, *33*, 2214627. DOI
110. Li, F.; Wang, D.; Xing, Q.; et al. Design and syntheses of MOF/COF hybrid materials via postsynthetic covalent modification: an efficient strategy to boost the visible-light-driven photocatalytic performance. *Appl. Catal. B. Environ.* **2019**, *243*, 621-8. DOI
111. Qin, J.; Dou, Y.; Zhou, J.; et al. Photocatalytic valorization of plastic waste over zinc oxide encapsulated in a metal-organic

- framework. *Adv. Funct. Mater.* **2023**, *33*, 2214839. DOI
112. Yu, Z.; Yang, Y.; Zhuang, H.; et al. In-situ growth of MIL-53 (Fe) on charcoal sponge as a highly efficient and recyclable photocatalyst for removal of Cr(VI). *Rare. Met.* **2024**, *43*, 4344-55. DOI
 113. Hussain, M. Z.; Yang, Z.; Huang, Z.; Jia, Q.; Zhu, Y.; Xia, Y. Recent advances in metal-organic frameworks derived nanocomposites for photocatalytic applications in energy and environment. *Adv. Sci.* **2021**, *8*, e2100625. DOI PubMed PMC
 114. Ren, X.; Wei, S.; Wang, Q.; et al. Rational construction of dual cobalt active species encapsulated by ultrathin carbon matrix from MOF for boosting photocatalytic H₂ generation. *Appl. Catal. B. Environ.* **2021**, *286*, 119924. DOI
 115. Liang, Q.; Gao, W.; Liu, C.; Xu, S.; Li, Z. A novel 2D/1D core-shell heterostructures coupling MOF-derived iron oxides with ZnIn₂S₄ for enhanced photocatalytic activity. *J. Hazard. Mater.* **2020**, *392*, 122500. DOI
 116. Wen, J.; Guo, Y.; Li, X.; et al. Photocatalytic Ag-MOF confers efficient antimicrobial activity to modified polyvinyl alcohol films. *Food. Biosci.* **2024**, *61*, 104959. DOI
 117. Kondo, Y.; Hino, K.; Kuwahara, Y.; Mori, K.; Yamashita, H. Photosynthesis of hydrogen peroxide from dioxygen and water using aluminium-based metal-organic framework assembled with porphyrin- and pyrene-based linkers. *J. Mater. Chem. A* **2023**, *11*, 9530-7. DOI
 118. Tran, V. A.; Sang, T. T.; Thu, N. A.; et al. Effect of pore structure in bismuth metal-organic framework nanorod derivatives on adsorption and organic pollutant degradation. *RSC. Adv.* **2024**, *14*, 31171-82. DOI PubMed PMC
 119. Tan, Y.; He, Y.; Yuan, D.; Zhang, J. Use of aligned triphenylamine-based radicals in a porous framework for promoting photocatalysis. *Appl. Catal. B. Environ.* **2018**, *221*, 664-9. DOI
 120. Yuan, J.; Wang, B.; Zong, Y.; Zhang, F. Ce-MOF modified Ceria-based photocatalyst for enhancing the photocatalytic performance. *Inorg. Chem. Commun.* **2023**, *153*, 110799. DOI
 121. Song, S.; Song, Z.; Han, H.; et al. Enhanced photocatalytic CO₂ reduction activity on the novel Z-scheme Co-MOF/Bi₂MoO₆ to form CO and CH₄. *Appl. Catal. A. Gen.* **2024**, *683*, 119834. DOI
 122. Chen, B.; Liu, L.; Song, Y.; et al. Functional upcycling of waste polyester into Cr-MOF towards synergistic interfacial solar evaporation and organic pollutant degradation. *Mater. Today. Sustain.* **2023**, *24*, 100561. DOI
 123. Akbarzadeh, E.; Soheili, H. Z.; Hosseini, M.; Gholami, M. R. Preparation and characterization of novel Ag₃VO₄/Cu-MOF/rGO heterojunction for photocatalytic degradation of organic pollutants. *Mater. Res. Bull.* **2020**, *121*, 110621. DOI
 124. Sun, X.; Yu, Q.; Zhang, F.; Wei, J.; Yang, P. A dye-like ligand-based metal-organic framework for efficient photocatalytic hydrogen production from aqueous solution. *Catal. Sci. Technol.* **2016**, *6*, 3840-4. DOI
 125. Tong, H.; Ji, Y.; He, T.; et al. Preparation and photocatalytic performance of UiO-66/La-MOF composite. *Water. Sci. Technol.* **2022**, *86*, 95-109. DOI
 126. Salehifar, N.; Zarghami, Z.; Ramezani, M. A facile, novel and low-temperature synthesis of MgO nanorods via thermal decomposition using new starting reagent and its photocatalytic activity evaluation. *Mater. Lett.* **2016**, *167*, 226-9. DOI
 127. Ebrahimi-Koodehi, S.; Ghodsi, F. E.; Mazloom, J. Ni/Mn metal-organic framework decorated bacterial cellulose (Ni/Mn-MOF@BC) and nickel foam (Ni/Mn-MOF@NF) as a visible-light photocatalyst and supercapacitive electrode. *Sci. Rep.* **2023**, *13*, 19260. DOI PubMed PMC
 128. Bai, Y.; Zhang, S.; Feng, S.; Zhu, M.; Ma, S. The first ternary Nd-MOF/GO/Fe₃O₄ nanocomposite exhibiting an excellent photocatalytic performance for dye degradation. *Dalton. Trans.* **2020**, *49*, 10745-54. DOI
 129. Javed, K.; Abbas, N.; Bilal, M.; et al. Fabrication of a ZnFe₂O₄@Co/Ni-MOF nanocomposite and photocatalytic degradation study of azo dyes. *RSC. Adv.* **2024**, *14*, 30957-70. DOI PubMed PMC
 130. Kim, J. H.; Wu, S.; Zdravil, L.; Denisov, N.; Schmuki, P. 2D metal-organic framework nanosheets based on Pd-TCPP as photocatalysts for highly improved hydrogen evolution. *Angew. Chem. Int. Ed.* **2024**, *63*, e202319255. DOI PubMed
 131. Pan, W.; Li, Z.; Qiu, S.; et al. Octahedral Pt-MOF with Au deposition for plasmonic effect and Schottky junction enhanced hydrogenothermal therapy of rheumatoid arthritis. *Mater. Today. Bio.* **2022**, *13*, 100214. DOI PubMed PMC
 132. Wang, X.; Li, H.; Song, Y.; Shi, Y.; Fan, J.; Cheng, L. Sn-MOF and Sn-MOF@Fe₃O₄ composites for highly efficient photocatalytic degradation of rhodamine B. *Polyhedron* **2024**, *255*, 117130. DOI
 133. Qiao, Y.; Chai, Y.; Jin, Q.; et al. A newly synthesized water-stabilized Zn-MOF for selective luminescent sensing of L-tryptophan and photocatalytic degradation of tetracycline. *J. Solid. State. Chem.* **2024**, *338*, 124873. DOI
 134. Hu, H.; Zhang, K.; Yan, G.; et al. Precisely decorating CdS on Zr-MOFs through pore functionalization strategy: a highly efficient photocatalyst for H₂ production. *Chin. J. Catal.* **2022**, *43*, 2332-41. DOI
 135. Zhang, X.; Ma, X.; Ye, Y.; et al. Enhanced photocatalytic hydrogen evolution with a Mixed-Valence iron Metal-Organic framework. *Chem. Eng. J.* **2023**, *456*, 140939. DOI
 136. Hu, J.; Lao, H.; Xu, X.; Wang, W.; Wang, L.; Liu, Q. In situ meso-tetra (4-carboxyphenyl) porphyrin ligand substitution in Hf-MOF for enhanced catalytic activity and stability in photoredox reactions. *Rare. Met.* **2024**, *43*, 2682-94. DOI
 137. Mao, S.; Shi, J.; Sun, G.; et al. Cu (II) decorated thiol-functionalized MOF as an efficient transfer medium of charge carriers promoting photocatalytic hydrogen evolution. *Chem. Eng. J.* **2021**, *404*, 126533. DOI
 138. Zhang, H.; Luo, Y. H.; Chen, F. Y.; Geng, W. Y.; Lu, X. X.; Zhang, D. E. Enhancing the spatial separation of photogenerated charges on Fe-based MOFs via structural regulation for highly-efficient photocatalytic Cr(VI) reduction. *J. Hazard. Mater.* **2023**, *441*, 129875. DOI PubMed
 139. Grape, E. S.; Flores, J. G.; Hidalgo, T.; et al. A robust and biocompatible Bismuth Ellagate MOF synthesized under green ambient

- conditions. *J. Am. Chem. Soc.* **2020**, *142*, 16795-804. DOI
140. Song, K.; Liang, S.; Zhong, X.; et al. Tailoring the crystal forms of the Ni-MOF catalysts for enhanced photocatalytic CO₂-to-CO performance. *Appl. Catal. B. Environ.* **2022**, *309*, 121232. DOI
141. Zhang, M.; Qin, Y.; Zhang, F.; et al. Site-selective etching and conversion of bismuth-based Metal-Organic frameworks by oxyanions enables efficient and selective adsorption via robust coordination bonding. *Chem. Eng. J.* **2024**, *488*, 150867. DOI
142. Hicks, K. E.; Wolek, A. T. Y.; Farha, O. K.; Notestein, J. M. The dependence of olefin hydrogenation and isomerization rates on zirconium metal-organic framework structure. *ACS. Catal.* **2022**, *12*, 13671-80. DOI
143. Ding, Z.; Li, X.; Kang, C.; et al. Single Ru atoms confined into MOF/C₃N₄ for dual improved photocatalytic carbon dioxide reduction and nitrogen fixation. *Chem. Eng. J.* **2023**, *473*, 145256. DOI
144. Li, L.; Lv, X.; Jin, L.; et al. Facile synthesis of Sn-doped MOF-5 catalysts for efficient photocatalytic nitrogen fixation. *Appl. Catal. B. Environ.* **2024**, *344*, 123586. DOI
145. Guo, X.; Yang, Z.; Zhao, J.; Liu, R. One-pot modulated construction of Ni-MOF/NiFe₂O₄ heterostructured catalyst for efficient oxygen evolution. *Rare. Met.* **2024**, *43*, 6751-7. DOI
146. Zhao, Z.; Bian, J.; Zhao, L.; et al. Construction of 2D Zn-MOF/BiVO₄ S-scheme heterojunction for efficient photocatalytic CO₂ conversion under visible light irradiation. *Chin. J. Catal.* **2022**, *43*, 1331-40. DOI
147. Zhao, Y.; Shen, J.; Yuan, J.; et al. Modulating electronic structures of MOF through orbital rehybridization by Cu doping promotes photocatalytic reduction of nitrate to produce ammonia. *Nano. Energy.* **2024**, *124*, 109499. DOI
148. Xu, J.; Lu, L.; Zhu, C.; et al. Insights into conduction band flexibility induced by spin polarization in titanium-based metal-organic frameworks for photocatalytic water splitting and pollutants degradation. *J. Colloid. Interface. Sci.* **2023**, *630*, 430-42. DOI
149. Shen, Y.; Yao, Y.; Lu, L.; et al. Insights into dual effect of missing linker-cluster domain defects for photocatalytic 2e⁻ ORR: radical reaction and electron behavior. *Chemosphere* **2023**, *324*, 138220. DOI
150. Zhao, Y.; Cui, H.; Hu, Y.; et al. A two dimensional hierarchically porous MOF-Cu with large lateral size via amino-groups regulated hydrolysis strategy and its superior photocatalytic reduction of CO₂. *Appl. Catal. B. Environ. Energy.* **2025**, *361*, 124567. DOI
151. Zhang, C.; Qin, S.; Gao, H.; Jin, P. High hydrogen evolution activities of dual-metal atoms incorporated N-doped graphenes achieved by coordination regulation. *J. Mater. Inf.* **2024**, *4*, 1. DOI
152. Xu, Y.; Ren, K.; Xu, R. In situ formation of amorphous Fe-based bimetallic hydroxides from metal-organic frameworks as efficient oxygen evolution catalysts. *Chin. J. Catal.* **2021**, *42*, 1370-8. DOI
153. Li, H.; Deng, C.; Li, F.; Ma, M.; Tang, Q. Investigation of dual atom doped single-layer MoS₂ for electrochemical reduction of carbon dioxide by first-principle calculations and machine-learning. *J. Mater. Inf.* **2023**, *3*, 25. DOI
154. Han, C.; Zhang, X.; Huang, S.; et al. MOF-on-MOF-derived hollow Co₃O₄/In₂O₃ nanostructure for efficient photocatalytic CO₂ reduction. *Adv. Sci.* **2023**, *10*, e2300797. DOI
155. Hua, J.; Wang, Z.; Zhang, J.; Dai, K.; Shao, C.; Fan, K. A hierarchical Bi-MOF-derived BiOBr/Mn_{0.2}Cd_{0.8}S S-scheme for visible-light-driven photocatalytic CO₂ reduction. *J. Mater. Sci. Technol.* **2023**, *156*, 64-71. DOI
156. Le, S.; Jin, Q.; Han, J.; et al. Rare earth element-modified MOF materials: synthesis and photocatalytic applications in environmental remediation. *Rare. Met.* **2024**, *43*, 1390-406. DOI
157. Li, Y.; Guo, Y.; Luan, D.; Gu, X.; Lou, X. W. D. An unlocked two-dimensional conductive Zn-MOF on polymeric carbon nitride for photocatalytic H₂O₂ production. *Angew. Chem. Int.* **2023**, *62*, e202310847. DOI
158. Isaka, Y.; Kawase, Y.; Kuwahara, Y.; Mori, K.; Yamashita, H. Two-phase system utilizing hydrophobic metal-organic frameworks (MOFs) for photocatalytic synthesis of hydrogen peroxide. *Angew. Chem. Int.* **2019**, *58*, 5402-6. DOI PubMed
159. Haris, M.; Khan, M. W.; Zavabeti, A.; Mahmood, N.; Eshtiaghi, N. Self-assembly of C@FeO nanopillars on 2D-MOF for simultaneous removal of microplastic and dissolved contaminants from water. *Chem. Eng. J.* **2023**, *455*, 140390. DOI
160. Zhang, Y.; Ma, F.; Ling, M.; Zheng, H.; Wu, Y.; Li, L. In-situ constructed indirect Z-type heterojunction by plasma Bi and BiO_{2-x}-Bi₂O₂CO₃ co-modified with BiOCl@Bi-MOF for enhanced photocatalytic efficiency toward antibiotics. *Chem. Eng. J.* **2023**, *464*, 142762. DOI
161. Dong, Q.; Li, X.; Sun, J.; et al. Regulating concentration of surface oxygen vacancies in Bi₂MoO₆/Bi-MOF for boosting photocatalytic ammonia synthesis. *J. Catal.* **2024**, *433*, 115489. DOI
162. Zhang, L.; Zhou, X.; Liu, S.; et al. Two birds, one stone: rational design of Bi-MOF/g-C₃N₄ photocatalyst for effective nitrogen fixation and pollutants degradation. *J. Clean. Prod.* **2023**, *425*, 138912. DOI
163. Lu, W.; Zheng, D.; Ye, D.; et al. N-heterocyclic carbene coordinated single atom catalysts on C₂N for enhanced nitrogen reduction. *J. Mater. Inf.* **2024**, *4*, 31. DOI
164. Xiao, S.; Pan, D.; Liang, R.; et al. Bimetal MOF derived mesocrystal ZnCo₂O₄ on rGO with high performance in visible-light photocatalytic NO oxidization. *Appl. Catal. B. Environ.* **2018**, *236*, 304-13. DOI
165. Ai, W.; Jiang, A.; Dong, X.; et al. An organic/inorganic Z-scheme heterojunction Yb-MOF/BiOBr for efficient photocatalytic removal of NO. *Mol. Catal.* **2024**, *559*, 114115. DOI